IEEE Access
Multidisciplinary | Rapid Review | Open Access Journal

Received 22 May 2024, accepted 23 June 2024, date of publication 28 June 2024, date of current version 8 July 2024.

Digital Object Identifier 10.1109/ACCESS.2024.3420426

TOPICAL REVIEW

Review on Multifunctional Pattern and Polarization Reconfigurable Antennas

VENKATASWAMY SURYAPAGA, (Student Member, IEEE), AND VIKAS V. KHAIRNAR, (Member, IEEE)
School of Electronics Engineering, VIT-AP University, Amaravati, Andhra Pradesh 522237, India
Corresponding author: Vikas V. Khairnar (vikas.vishnu@vitap.ac.in)

This work was supported by the Vellore Institute of Technology Andhra Pradesh (VIT-AP) University.

ABSTRACT This paper presents a detailed review of multifunctional pattern and polarization reconfigurable antennas, highlighting their potential to enhance performance of the wireless communication systems. These adaptable antennas offer versatile functionalities, eliminating the need for multiple antennas. The review provides a comprehensive overview of various techniques used to achieve reconfiguration, including electrical, optical, physical, and smart materials-based methods. It discusses the advantages, limitations, and practical considerations associated with each technique. The paper also explores the applications of reconfigurable antennas across diverse domains such as wireless LAN system, 5G communication, cellular network, underground mining, MIMO system, electromagnetic imaging, satellite communication, and cognitive radio. The review includes a comparative study between pattern reconfigurable antennas and multifunctional pattern and polarization reconfigurable antennas. The multifunctional pattern and polarization reconfigurable antennas are categorized into pattern reconfigurable antennas radiating in different directions, beam steering antennas with linear polarization reconfiguration, beam steering antennas with circular polarization reconfiguration, and beam steering antennas with both linear and circular polarization reconfigurations. Finally, challenges and future research directions in the design of multifunctional pattern and polarization reconfigurable antennas are discussed.

INDEX TERMS Reconfigurable antenna, pattern reconfigurable antenna, beamwidth reconfigurable antenna, pattern and polarization reconfigurable antenna.

I. INTRODUCTION

Future wireless communication systems demand antennas with multifunctional capabilities, adaptability, and flexibility. Reconfigurable antennas offer a solution to overcome the limitations of conventional antennas, which are typically designed for specific applications with fixed operating parameters [1]. Unlike conventional antennas, reconfigurable antennas can adjust their operating parameters in real-time based on specific requirements. This capability is highly advantageous for next-generation wireless communication applications. A single reconfigurable antenna can replace multiple single-function antennas, resulting in a reduction in overall size, cost, and complexity of a system, while simultaneously enhancing performance [2].

Reconfigurable antennas are classified according to the parameter which is reconfigured such as frequency [3], pattern [4], polarization [5], and compound [6], [7], [8], [9], [10], [11], [12], [13], [14], [15] reconfiguration. Fig. 1 illustrates classification of reconfigurable antennas. Compound reconfigurable antennas are classified based on their ability to simultaneously reconfigure two or more parameters such as frequency and pattern [6], [7], [8], [9], frequency and polarization [10], [11], pattern and polarization [12], and frequency, pattern and polarization [13], [14], [15]. Multifunctional antennas can have capabilities of frequency reconfiguration, polarization reconfiguration, and radiation pattern reconfiguration in a single antenna structure. Combination of a couple of these features makes these antennas multifunctional. These antennas are capable of adapting to various wireless communication standards and support a wider range of applications [16].

The associate editor coordinating the review of this manuscript and approving it for publication was Giorgio Montisci.

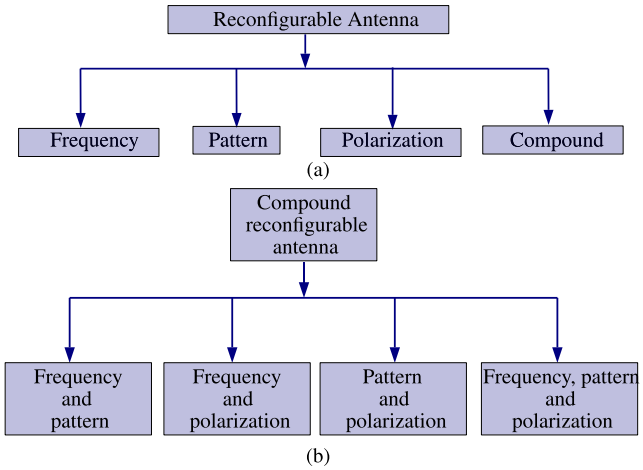

FIGURE 1. Classification of (a) Reconfigurable antenna and (b) Compound reconfigurable antenna.

Frequency reconfiguration is typically achieved by changing the path of electrical currents on the antenna structure. This causes variation in the electrical length of resonant antennas. Frequency reconfigurable antennas possess the capability to modify their operating band in accordance with the availability of the spectrum and adapt to dynamic environmental conditions [3]. Frequency reconfigurable antennas are divided into two main categories: continuous tuning [17] and discrete switching [18]. Continuous tunable frequency reconfigurable antenna allows for smooth transition between operating bands, while discrete frequency reconfigurable antenna offers operation at specific frequency bands.

Pattern reconfigurable antennas enhance coverage by effectively avoiding noise sources. This is achieved by directing nulls towards interfering signals while focusing the main beam towards the desired direction [4]. These antennas can radiate in different directions and produces different beam shapes. Additionally, they can achieve beam steering and beamwidth reconfigurability within a single antenna structure.

Polarization reconfigurable antenna helps to avoid multipath fading and double the communication capacity by utilizing frequency reuse technology [5]. Polarization of an antenna is classified into three categories as linear, elliptical, and circular. Linear polarization (LP) is further classified as linear horizontal polarization (LHP) and linear vertical polarization (LVP). Circular polarization (CP) is divided into two categories as right-hand CP (RHCP) and left-hand CP (LHCP). Polarization reconfiguration can occur between different types of LP, different types of CP, or between LP and CP.

The design and implementation of reconfigurable antennas come with a set of challenges. The impedance characteristics of antennas are closely linked to their radiation characteristics. The frequency reconfiguration has an impact on radiation characteristics and radiation pattern reconfiguration will alter the antennas frequency response [19]. The primary objective of a reconfigurable antenna designer is to have the capability to independently choose the operating frequency, bandwidth, and radiation characteristics. It is challenging to attain compound reconfigurability with simple biasing circuit [20]. In the last decade, many pattern reconfigurable and polarization reconfigurable antennas with exceptional performance characteristics are presented in the literature. However, polarization of most of the pattern reconfigurable antennas is fixed. Similarly, most polarization reconfigurable antennas has fixed radiation characteristics. It is observed that very few antenna designs are capable of realizing independent pattern and polarization reconfiguration in a single antenna structure. Multifunctional antennas that reconfigure both pattern and polarization hold immense potential to improve communication system performance [21], [22], [23].

In the past some efforts have been made to review the existing work on reconfigurable antennas [2], [24], [25], [26], [27], [28]. The present review is focused on antenna designs realizing independent pattern and polarization reconfigurability. The multifunctional pattern and polarization reconfigurable antennas are classified according to their pattern reconfiguration capabilities such as beam direction and beam switching or steering.

The key contribution of this article is as follows:

- The article provides a comprehensive overview of the various techniques employed to achieve reconfiguration in antennas. It also includes a thorough discussion of the advantages and disadvantages of each method.
- This article explores the potential of multifunctional antennas for next-generation wireless communication systems, focusing on performance metrics and experimental data.
- This article presents a comprehensive classification of multifunctional pattern and polarization reconfigurable antennas based on their radiation characteristics. It also provides a thorough review and detailed performance comparison of reconfigurable antenna designs that achieve independent pattern and polarization reconfiguration.
- The article also presents limitations, challenges, and future research directions for state-of-the-art multifunctional pattern and polarization reconfigurable antennas.
- The review will assist the antenna designers to select the appropriate design techniques to achieve independent pattern and polarization reconfiguration for a specific application.

The remaining sections of the paper are organized as follows: Section II explores the various techniques used to achieve reconfiguration. In Section III applications of reconfigurable antennas are discussed. Classification of pattern reconfigurable antennas is presented in Section IV. This also includes a comprehensive discussion of the techniques utilized to achieve pattern reconfiguration in antennas. Section V discusses few reported works on polarization reconfigurable antennas. Section VI presents detailed performance comparison of multifunctional

pattern and polarization reconfigurable antennas. Comparative analysis of the reported multifunctional pattern and polarization reconfigurable antennas is presented in Section VII. Section VIII presents emerging trends and future research directions. Concluding remarks are given in Section IX.

II. TECHNIQUES USED TO ACHIEVE RECONFIGURATION

This section presents a detailed discussion on techniques used to achieve reconfiguration in antennas. Reconfigurable antennas are implemented using six major types of reconfiguration techniques, as shown in Fig. 2. These techniques include electrical switches, optical switches, mechanical movement, and smart material-based approaches. The implementation challenges associated with the PIN diodes and varactor diodes are also discussed in detail. Additionally, challenges encountered in the millimeter-wave (mm-wave) frequency ranges are also highlighted.

A. ELECTRICAL RECONFIGURATION

In electrically reconfigurable antennas, different RF switches such as PIN diode, varactor diode, field effect transistor (FET), and micro-electro-mechanical systems (MEMS) are employed to redirect surface current on the antenna structure. Fig. 3 shows equivalent circuit representation for the PIN diode in on and off state. The on state of the PIN diode is equivalently represented by considering a series combination of resistor R_f and inductor L_f. Off state of the PIN diode is modeled by a parallel combination of resistor R_p and capacitor C_p in series with inductor L_f. When the PIN diode is in on state, it offers low impedance, enabling the RF signal to pass through. Conversely, when it is in the off state, it presents high impedance, effectively blocking the RF signal. By varying the bias voltage applied to a PIN diode, its intrinsic resistance can be controlled, allowing for variable RF attenuation. This property is essential in applications where precise control over signal levels is necessary. PIN diodes are commonly employed in phase shifters, where the phase of an RF signal can be controlled by varying bias voltage of the PIN diode. This capability is particularly useful in phased array antennas and other beamforming systems. Moreover, in some cases, PIN diodes can be used for frequency tuning by changing the capacitance of a resonant circuit. The utilization of PIN diodes presents various benefits, including a high power handling capacity, minimal insertion loss while in the deactivated state. Nevertheless, they do come with a set of challenges, such as relatively slow switching speeds, complex control circuitry demands, and limitations in adapting to a wide range of frequencies.

Varactor diodes are commonly utilized in RF and microwave systems for reconfiguration, enabling frequency tuning in oscillators, filters, and resonant circuits by varying their capacitance with applied reverse voltage. Fig. 4 presents equivalent circuit representation for the varactor diode consisting of series combination of resistor R_s, inductor L_p, and variable capacitor C_j. Varactor diodes offer several

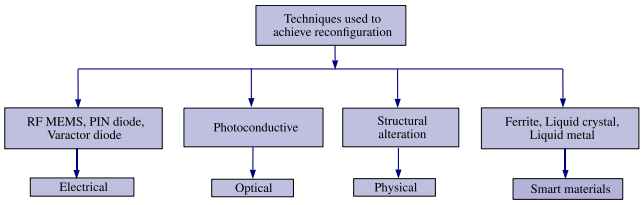

FIGURE 2. Various techniques adopted to achieve reconfiguration in antennas [43].

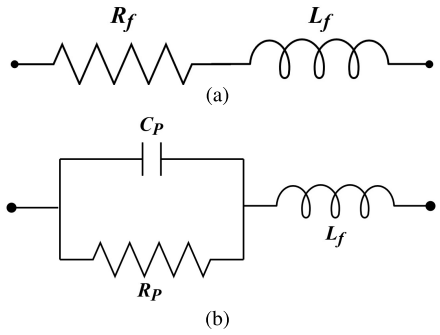

FIGURE 3. Equivalent circuit representation for the PIN diode in (a) On state and (b) Off state.

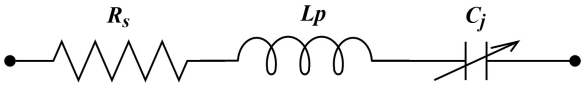

FIGURE 4. Equivalent circuit model representation of the varactor diode.

advantages over PIN diodes, notably a larger tuning range, lower control voltage requirements, and increased switching speeds. Nevertheless, they also exhibit certain limitations, including high insertion loss that can influence efficiency of antenna radiation, non-linear behavior, and constraints on their power handling capacity. On the other hand, MEMS switches boast numerous advantages when compared to PIN diodes and varactor diodes, encompassing rapid switching speeds, minimal insertion loss, and high linearity. However, MEMS switches are accompanied by numerous fabrication challenges and complex control circuits [29]. Table 1 summarizes the PIN diodes and varactor diodes employed in the design of multifunctional pattern and polarization reconfigurable antennas [13], [14], [20], [30], [31], [32], [33], [34], [35], [36], [37], [38], [39], [40], [41], [42]. The table provides details including model, manufacturer, and key electrical parameters of these diodes.

1) IMPLEMENTATION CHALLENGES

The implementation of PIN diodes and varactor diodes presents notable challenges that impact performance of the reconfigurable antennas. In simulations, diodes are typically represented using an equivalent lumped circuit model. However, these values are specific to a single operating frequency and may not remain consistent at other frequencies, causing discrepancies between simulated and

TABLE 1. Details of PIN diodes and varactor diodes used in the design of multifunctional pattern and polarization reconfigurable antennas.

Ref.	Model	Company	Value	Physical form
[30]	SMP1320-079LF	Skyworks solutions	R_{on} = 0.75 Ω C_{off} = 0.23 pF	
[14]	BAR50-02L	Infineon technologies	R_{on} = 16.5 Ω C_{off} = 0.2 pF	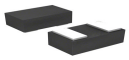
[31]	BAR50-02L	Infineon technologies	R_{on} = 2 Ω, L = 0.4 nH R_{off} = 5.5 kΩ, C_{off} = 0.1 pF	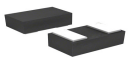
[32]	BAR50-02L	Infineon technologies	R_{on} = 2.1 Ω, L = 0.6 nH R_{off} = 3 kΩ, C_{off} = 0.15 pF	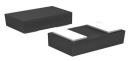
[13]	NXP BAP64-02	NXP semiconductors	R_{on} = 3 Ω R_{off} = 2.6 kΩ, C_{off} = 0.28 pF	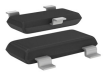
[33]	SMV 1233-079LF	Skyworks solutions	R_s = 1.2 Ω, L = 0.7 nH C = 0.84 to 5.08 pF	
[34]	BAR50-02V	Infineon technologies	R_{on} = 3 Ω R_{off} = 5 kΩ, C_{off} = 0.15 pF	
[35]	BAR64-03W	Infineon technologies	R_{on} = 2.1 Ω, L = 1.8 nH R_{off} = 300 kΩ, C_{off} = 0.2 pF	
[36]	BAR64-03W	Infineon technologies	R_{on} = 2.1 Ω, L = 1.8 nH R_{off} = 3 kΩ, C_{off} = 0.17 pF	
[37]	BAR50-02L	Infineon technologies	R_{on} = 1.2 Ω, L = 0.4 nH R_{off} = 5 kΩ, C_{off} = 0.15 pF	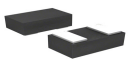
[38]	SMV1405-079LF	Skyworks solutions	R_s = 0.8 Ω, L = 0.7 nH C = 0.63 to 2.67 pF	
[39]	MADP-000907-14020	MACOM	R_{on} = 5.2 Ω C_{off} = 0.025 pF	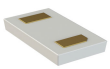
[40]	BAR50-02V	Infineon technologies	R_{on} = 1.5 Ω, L = 0.7 nH R_{off} = 5 kΩ, C_{off} = 0.3 pF	
[20]	MADP-000907-14020	MACOM	R_{on} = 5.2 Ω, L = 0.4 nH R_{off} = 5 kΩ, C_{off} = 0.03 pF	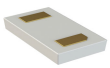
[41]	SMP1345-040LF	Skyworks solutions	R_{on} = 1.5 Ω, L= 0.45 nH C_{off} = 0.19 pF	
[42]	DSM8100-000	Skyworks solutions	R_{on} = 4 Ω R_{off} = 20 kΩ, C_{off} = 0.03 pF	

measured results [44]. To address this issue, researchers often extract the scattering parameters of PIN diodes from their datasheet and incorporate them into simulation environments to enhance performance accuracy [45]. An in-depth analysis conducted in [46] examines the impact of electronic switching components on antenna performance.

Two different electronic implementations are evaluated, and their performance is compared to an ideal scenario where switch states are modeled as perfect open and short circuits. Under forward biased conditions, series resistance is considered to address the insertion loss of the PIN diode. Conversely, under reverse bias conditions, the diode is modeled considering capacitance, which accounts for the parasitic coupling between the diode terminals. In the first configuration, a single PIN diode is utilized, while in the second configuration, two diodes are linked with the anode serving as the shared terminal. Each configuration employs two distinct diodes: Skyworks SMP1345 and SMP1322. The study concludes that the choice of equivalent capacitance (C_T) during reverse biased configuration notably impacts the antennas front-to-back ratio. Furthermore, it is observed that opting for higher C_T values leads to significantly poorer performance. Low capacitance diodes can be employed, but they come with higher series resistance values when in forward biased mode, which impacts the antennas radiation efficiency. Increased series resistance values lead to greater losses, consequently lowering the antennas radiation efficiency.

In [47], a 1-bit reconfigurable reflectarray is equipped with Skyworks SMP1340 PIN diodes to achieve ±60° monopulse beam steering. Reflective phase shift measurement is employed to obtain an accurate and precise model of the PIN diodes through two iterative design loops. The component values obtained from the datasheet are inaccurate, resulting in frequency shift and phase error. The parameters obtained from the datasheet are as follows: $L_{ON} = 600$ pH, $R_{ON} = 1\ \Omega$, $C_{OFF} = 180$ fF, $L_{OFF} = 600$ pH, and $R_{OFF} = 10\ \Omega$. The parameters extracted after the two iterative design loops are as follows: $L_{ON} = 450$ pH, $R_{ON} = 1\ \Omega$, $C_{OFF} = 100$ fF, $L_{OFF} = 450$ pH, and $R_{OFF} = 10\ \Omega$. Similarly, in [48], the S-parameters of SMV2020 varactor diodes are measured to determine actual values of series resistance (R_s), parasitic inductance (L_p), and junction capacitance (C_j). This step is crucial as datasheet typically provide average values at specific frequencies, which may not accurately represent the diodes behavior across different frequencies. Subsequently, the antenna is simulated using these measured parameter values to ensure better agreement between simulated and measured results. Moreover, in [49], a microstrip through-reflect-line calibration setup is employed to accurately characterize the MACOM PIN diode MADP-000907-14020. This involves mounting the diode inside a 0.2 mm gap of a microstrip line with a width of 0.3 mm. Such detailed characterization processes are essential for improving the reliability of parameter values, thereby enhancing simulation accuracy and overall antenna performance.

An alternative method for modeling reactive elements using simulation program with integrated circuit emphasis (SPICE) in circuit co-simulations is presented in [50]. This modeling technique is explored through the development of a varactor-loaded active frequency selective surface (FSS)-based tunable absorber. The modeling process involves conducting numerical simulations of the unit cell using Ansys HFSS, coupled with a co-simulation that incorporates the SPICE model of the varactor diode through Ansys Circuit Design. Subsequently, the S-parameter data of the unit cell model is extracted from the full-wave EM simulator HFSS and then imported into the circuit simulations. Here, the SPICE model of the varactor diode is seamlessly integrated with the extracted S-parameter data. This method diverges from the conventional practice of using equivalent lumped circuits, as it enables the direct integration of SPICE model parameters of a reactive component into full-wave EM solvers, thereby accurately replicating its device characteristics.

2) CHALLENGES AT MILLIMETER-WAVE (MM-WAVE) FREQUENCIES

The frequency bands around 28 GHz, 38 GHz, 60 GHz, and 73 GHz are considered for indoor and outdoor communication at mm-wave frequency range [51]. However, while reconfigurable antennas are common at microwave frequencies, achieving reconfiguration at mm-wave frequencies presents challenges. This is largely due to the suboptimal performance of electrical switching elements at these higher frequencies. Using electrical switching elements like PIN diodes and varactor diodes in the mm-wave frequency range presents several difficulties. These include increased losses and a significant packaging volume relative to the wavelength. Additionally, the active components require a specialized biasing circuit design, which increases antennas overall size [52]. It is noted that at mm-wave frequencies, a more accurate model of the switching elements must consider the parasitic effects of the switching elements. In [53], detailed comparison of electrical switching elements such as PIN diode, RF MEMS, and FET operating at mm-wave frequencies is presented. It is worth mentioning that only a limited number of PIN diodes function effectively in this frequency range, often resulting in higher losses [54], [55]. To address the challenges of electrical switching components at mm-wave frequencies, one can utilize smart materials like liquid crystals, graphene, and phase change materials [52], [56].

Based on the detailed analysis of electrical reconfiguration techniques, this section summarizes that,

- One advantage of the electrical switching technique is the ease of integrating the active elements directly into the antenna structure. However, separate biasing circuit needs to be designed for activation of switching elements and isolation of RF and DC signals. To ensure low power consumption and minimal impact on the radiation characteristics of antennas, it is important to design the biasing circuit with a few bypass capacitors and choke inductors [57].
- The use of electrical switching elements, such as PIN diodes and varactor diodes, significantly affects the antennas gain and radiation efficiency. The gain

and radiation efficiency of the antenna can experience degradation, primarily due to increased I^2R losses stemming from the generation of high currents within the antenna elements [58]. To significantly enhance the radiation efficiency of reconfigurable antennas, it is essential to employ low loss microwave substrates and high quality diodes with minimum ohmic losses [59].

- It is an ideal approach to design reconfigurable antennas with a minimum number of active components. This approach promotes the creation of simple control circuit designs, reduced power consumption, and improved overall radiation efficiency. In general, reconfigurable antenna designs characterized by straightforward biasing and control circuits can be seamlessly integrated with other communication devices and subsystems. In contrast, designs incorporating numerous active components and intricate biasing circuits can encounter issues during the testing and validation phase.
- The selection of electrical switches for reconfigurable antennas should be tailored to the specific demands of the application, operational frequency, and switching speed requirements. It is necessary to select proper reconfiguration technique as per the constraints imposed by the application for which the antenna is designed.

B. OPTICAL RECONFIGURATION

The optically controlled reconfigurable antenna utilizes photoconductive switching elements activated by laser light [60], [61], [62], [63]. The first optically reconfigurable antenna operating in the mm-wave frequency band is presented in [60]. This antenna incorporates a slotted-waveguide antenna array and two photoconductive switches to regulate the electrical length of the slots. By utilizing these switches, the antenna achieves minimal insertion loss, as the photoconductive elements are strategically placed to adjust the slot length without directly interfering with the antennas switching path. In [61], a frequency reconfigurable antenna design employs photoconductive switches, providing excellent isolation between optical and microwave signals and enabling high speed switching. The research also addresses optimizing the frequency switching ratio while considering finite photoconductance, revealing a trade-off between switching ratio and minimum photoconductance. Additionally, [62] introduces a frequency reconfigurable antenna utilizing an organic semiconductor polymer P3HT as the radiating patch. Frequency reconfiguration is achieved by varying the intensity of optical illumination aimed at the P3HT from a white light source. Comparatively, the P3HT-based antenna exhibits moderate radiation efficiency and lower gain when compared to a traditional copper microstrip antenna. The optical reconfiguration technique offers several benefits such as low loss, reduced interference from biasing lines, low power consumption, and avoidance of radiation pattern distortion, as it eliminates the need for complicated biasing circuits. Nevertheless, they have certain limitations compared to electrical reconfiguration, including complex implementation, high cost, integration issues, and increased system size. Precise control over laser activation is crucial in this technique, requiring regular calibration for optimal performance, and consideration of overall power requirements, including those for the laser source.

C. PHYSICAL RECONFIGURATION

The physical reconfiguration technique involves structural alteration of the antenna radiating parts [64], [65], [66], [67], [68]. A polarization reconfigurable antenna is described in [66], consisting of an L-probe feed on the bottom substrate and a truncated corner patch on the upper substrate. The polarization states are controlled by rotating the patch relative to the capacitively coupled feed. The study concludes that employing physical rotation in reconfigurable antennas is suitable when cost effectiveness and quick fabrication are prioritized over switching speed. A pattern reconfigurable antenna based on metasurface presented in [67] utilizes mechanical rotation. The antenna consists of a circular patch on a lower substrate and a semi-circular metasurface on the top substrate. The metasurface is rotated relative to the source antenna to achieve beam steering. The mechanically pattern reconfigurable antenna presented in [68] achieves beamwidth reconfigurability suitable for high power applications. This antenna features an H-sectoral horn antenna with two movable metallic flaps. The study concludes that employing the electrical switching technique for pattern reconfiguration is a viable solution. However, it is noted that the use of electrical switching components imposes limitations on the antennas power handling capacity. Consequently, the results suggest that employing mechanical pattern reconfigurability is the optimal solution for high power applications. The physical reconfiguration method does not depend on any switching mechanism and laser diode integration. While this method offers excellent control capabilities, its application is limited to scenarios where reconfiguration speed is low. It is noted that structural modification of antenna parts increases size, cost, complexity, and power source requirements of the overall system. Implementing a dependable and accurate control system is vital for achieving the desired reconfiguration outcomes. Additionally, environmental factors such as temperature, humidity, and mechanical vibrations can impact performance of the physically reconfigurable antennas.

D. SMART MATERIALS BASED RECONFIGURATION

Smart materials such as liquid crystals [69] and ferrite [70] can be employed to make antennas reconfigurable, enabling them to adapt and change their properties as needed. The characteristics of liquid crystal and ferrite can be changed by applying an external voltage and static electrical field. Liquid crystals can be used at optical as well as microwave frequencies. Their power consumption is relatively low, however, they have to be kept at the temperature range between 20°C to 35°C in order to stay in the liquid crystal state. The ferrite based reconfigurable antennas has the

advantage of antenna miniaturization and wide tuning range. However, they are associated with complex biasing network and high DC power consumption. The main disadvantage associated with this technique is the low efficiency of these materials at microwave frequencies.

Liquid metal-based antennas have emerged as a promising solution for achieving reconfiguration, overcoming the limitations of electrically switching active devices such as complex control circuits and increased ohmic losses [71], [72], [73], [74], [75], [76], [77], [78], [79]. The liquid metal has the advantages of low insertion loss, linear behavior, high power handling capacity, low harmonic distortion, large tuning ranges, and can be mechanically or chemically translated, stretched, and relaxed to obtain more operating configurations. In [74], a pattern reconfigurable antenna design is proposed, employing a polymethyl methacrylate substrate with nested microfluidic channels. Liquid metal injected into specific zones within the substrate enables pattern reconfiguration. To enhance elasticity and toughness, liquid metal antennas utilize eutectic gallium-indium (EGaIn) alloy, which remains liquid at room temperature to achieve pattern reconfiguration [75]. The antenna design presented in [76] utilizes parasitic elements and a switchable ground plane to achieve pattern reconfiguration. Control over the parasitic elements is attained by filling or emptying drill holes with liquid metal. Moreover, liquid metal is also employed to achieve compound reconfiguration. A frequency and polarization reconfigurable antenna presented in [77], utilizes eutectic gallium-indium (EGaIn, 75% gallium, 25% indium, conductivity of 3.4×10^6 S/m).

Liquid metal-based antennas offer several advantages over conventional mechanical switch control methods, including good fluidity, flexible controllability, elimination of complex biasing circuits, and the possibility of continuous tuning. The flow of liquid within the fluidic channel is regulated through various methods such as air pump, syringe injection, and electrochemical processes. However, discrepancies between simulated and measured results in liquid metal-based antennas have been observed. Factors contributing to these variations include unbalanced distribution of channel material, reduction in conductive effect, and the impact of NaOH solution on overall radiation efficiency. The frequency and polarization reconfigurable antenna design presented in [78] utilizes gravity to control self-circulation of liquid metal. A polydimethylsiloxane (PDMS) structure with a square ring channel is integrated onto the microstrip antenna. Gravity regulates the contact position between the liquid metal and the patch facilitating conditions for reconfiguration. The non-linear characteristics of semiconductor devices employed for reconfiguration lead to the generation of intermodulation distortion (IMD), which is undesirable for many practical applications [79]. Liquid metal-based devices, in contrast, demonstrate superior handling of higher power and exhibit a better response when compared to semiconductor-based active devices. To assess the distortion generated, an experimental investigation is conducted comparing varactor-tuned monopoles with liquid metal monopoles. The results indicate that electrochemically controlled capillary-based reconfigurable liquid metal monopoles exhibit superior linearity in comparison to varactor-tuned monopoles.

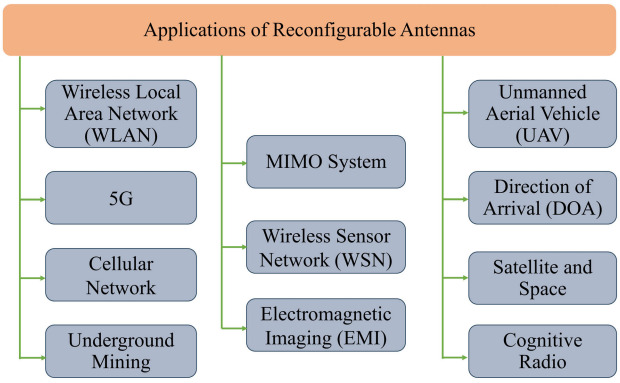

FIGURE 5. Applications of reconfigurable antennas [16], [19].

III. APPLICATIONS OF RECONFIGURABLE ANTENNAS

The utilization of reconfigurable antennas holds the potential to enhance the performance of wireless communication applications. In this section, we delve into a detailed analysis of the advantages provided by reconfigurable antennas across diverse applications, examining performance indicators and experimental outcomes. Applications of reconfigurable antennas are illustrated in Fig. 5.

A. WIRELESS LOCAL AREA NETWORK (WLAN) SYSTEM

The pattern reconfigurable antenna proposed in [80] aims to function within the frequency range of IEEE 802.11 b/g. The primary beam of this antenna with pattern reconfigurability can be switched discretely to a 30° angle in the vertical plane for each azimuthal direction, with a switching interval of 45°. A system-level experimental analysis is conducted on a wireless local area network (WLAN) system operating at a carrier frequency of 2.5 GHz, utilizing a 10 MHz signal bandwidth. The experimental setup comprises of a WLAN system with two nodes: node A equipped with an omnidirectional antenna and node B utilizing multifunctional reconfigurable antenna.

Performance of the multifunctional reconfigurable antenna is tested in a typical indoor environment and is compared with an omnidirectional antenna, with key performance metrics of effective signal-to-noise ratio (SNR), achievable data rate, and bit error rate (BER). Initially, a SNR gain is attained through the utilization of both the multifunctional reconfigurable antenna and an omnidirectional antenna, considering various orientations including opposite orientation, side-to-side orientation, and face-to-face orientation. Notably, the face-to-face orientation of the multifunctional reconfigurable

antenna demonstrates an approximate 10 dB performance improvement compared to the omnidirectional antenna. Moreover, the effective SNR is computed across different transmit power levels, revealing that the multifunctional reconfigurable antenna consistently achieves an average SNR gain of 5 to 6 dB in comparison to omnidirectional antenna systems. The attainable data rate is assessed under varying transmit power levels, and the results indicate that the multifunctional reconfigurable antenna based system achieves an additional data rate of approximately $\sim$ 2 bits/sec/Hz compared to omnidirectional antenna systems.

B. FIFTH GENERATION (5G) COMMUNICATION

The 5G wireless communication network promises to deliver a higher data rate, more reliable service, and improved coverage. A pattern reconfigurable antenna has been designed to meet the specific needs of 5G technologies [81]. It possesses the capability to perform joint beam steering and adjust the beamwidth as required. The proposed reconfigurable antenna generates nine modes for beam steering and three modes for beamwidth reconfigurability. A control algorithm is also proposed to select the optimal operating mode of operation concerning dynamic variations in the wireless communication channel.

Performance of the reconfigurable antenna is experimentally verified within a 5G cellular system employing orthogonal frequency division multiplexing (OFDM) for its transmission. Two distinct spatial user deployment scenarios are considered a) In the uniform user density scenario, users are uniformly distributed across the coverage area and b) In the hotspot deployment scenario, users are situated within a radius of 20 meters from cluster centers, which themselves are randomly distributed in space. Performance of the proposed antenna is compared with systems utilizing conventional patch antennas. It is concluded that reconfigurable antenna with pattern and beamwidth reconfiguration provides 29% coverage and 16% capacity gain improvement as compared to the conventional patch antennas.

C. CELLULAR NETWORK

Performance of the pattern reconfigurable antenna is analyzed in a hexagonal homogeneous cellular network to improve cell edge performance [82]. The complete antenna assembly consisting of dipole as a radiating element and metallic reflectors is placed around the base station in three sector configuration. The analysis is carried out to find the trade-offs associated with antenna beamwidth variations within a uniform cellular deployment. Objectives for the analysis is to enhance available capacity for users at the cell periphery and optimizing the average user capacity. Factors such as mechanical tilt, inter-site distance, path loss models, and proximity to cell edges exert their influence on these considerations. A reconfigurable antenna is simulated and evaluated at a 1.9 GHz frequency, which corresponds to the usual frequencies used in cellular networks. The system analysis is performed using the azimuth beam switching method by varying beamwidth of the antenna between 50° to 180°. The numerical analysis results demonstrates that by adjusting the beamwidth of pattern reconfigurable antenna from 60° to 110°, the antenna configuration can achieve a 20% improvement in the typical cell edge capacity.

D. UNDERGROUND MINING

Performance of the pattern reconfigurable antenna is investigated in underground mining for both line-of-sight (LOS) and non-line-of-sight (NLOS) propagation scenarios to improve wireless communication link [83]. The fixed performing antennas are unable to tackle the difficulties of dynamic variation in channel conditions. Experimental evaluations are conducted to capture the complex channel impulses when using both a conventional antenna and a reconfigurable antenna. The findings indicate that, in environments with significant multipath interference, the reconfigurable antenna ensures a more reliable connection. For the LOS setup, the influence of both distance and tunnel design on the reconfigurable antenna is analyzed. In contrast, in the NLOS context, the reconfigurable antennas effectiveness is analyzed with varying tunnel sizes. A comparative analysis between the reconfigurable antenna and the dipole is undertaken for both LOS and NLOS scenarios, focusing on path loss and delay spread. The experimental results demonstrate that as compared to fixed performing antenna, the pattern reconfigurable antenna attains 20% and 34% improvement in path loss and delay spread, respectively.

E. MULTIPLE INPUT MULTIPLE OUTPUT (MIMO) SYSTEM

The increasing demand for wireless data has prompted the development of new technological solutions to meet the high performance requirements. In particular, multiple input multiple output (MIMO) antenna systems have become an essential component of modern wireless devices, playing a crucial role in improving data throughput and ensuring a high quality of service. The utilization of reconfigurable antennas in MIMO systems offers the potential for increased capacity, thereby enhancing the overall reliability and robustness of wireless links.

In [21], performance of pattern and polarization reconfigurable antenna is investigated for narrowband and broadband MIMO systems. The advantages provided by reconfigurable antennas are examined in both LOS and NLOS scenarios. The pattern reconfiguration is achieved by stimulating higher order modes within a two port circular patch antenna. On the other hand, polarization reconfiguration is attained by adjusting the phase shift between two orthogonal modes generated on the same circular patch. The experimental analysis is carried out in an indoor environment consisting of reconfigurable antennas at one or both ends of the communication link. The experimental analysis shows that the pattern and polarization reconfiguration improves

diversity level of the MIMO system. As a result, a capacity improvement of 17.5% is achieved in a narrowband channel. The reconfigurable antennas shows significant improvement in the channel capacity as compared with the conventional circular patch antenna elements.

F. WIRELESS SENSOR NETWORK (WSN)

Conventionally, monopole and dipole antennas with an omnidirectional radiation pattern are used in wireless sensor network (WSN) nodes. However, pattern reconfigurable antennas offer significant performance enhancements over omnidirectional antennas in terms of energy consumption, communication range, and signal sensitivity. Furthermore, the ability of pattern reconfigurable antennas to adapt to the surrounding radio environment enables them to optimize their receiving characteristics for improved performance. In [84], a parasitic slot antenna array is introduced and its performance is evaluated through experimentation on a sensor network system. To explore the effects of the electronically adjustable antenna integrated into the manhole cover within the operational sensor system, it is assessed in situations where communication is previously compromised at two specific nodes. The measurements indicate that the pattern reconfigurable antenna enhances the packet reception rate by 64% and increases the received signal strength by 10 dB in comparison to the uniformly radiating dipole antenna.

G. ELECTROMAGNETIC IMAGING (EMI)

Reconfigurable antennas are crucial in electromagnetic imaging (EMI) systems for detecting fluid presence in the torso [85]. In this study, a metasurface antenna capable of pattern reconfiguration is proposed to construct an EMI system. Operating within the 0.8 to 1.05 GHz frequency range, this antenna allows for steering the main beam from $-30°$ to $30°$, enabling scanning of the human chest with controllable unidirectional radiation patterns. To verify the antennas practicality, it is employed within a realistic electromagnetic imaging setup. The antenna is positioned in front of an artificial torso model with a chest circumference of 94 cm, containing major cardiovascular organs like the heart, lungs, ribs, and adipose tissue. To simulate fluid accumulation in the torso, 20 ml of water is introduced into the phantom's lungs. In order to capture information from all perspectives around the torso, the torso model is rotated in steps of $22.5°$, while the antenna remains stationary to gather data from 16 different positions. For each angle of rotation, the antenna scans chest area by altering its radiation pattern in three distinct directions, designated as mode 1, mode 2, and mode 3. The scattering parameters corresponding to these modes, obtained from various sections of the torso, are collected using a vector network analyzer (VNA). The system is able to identify the presence of 20 ml of fluid within the torso, thus enabling differentiation between healthy and unhealthy cases.

H. UNMANNED AERIAL VEHICLE (UAV)

A test environment is presented for assessing the effectiveness of unmanned aerial vehicle (UAV) in aerial to ground communication links [86]. The testbed comprises a software defined radio (SDR) and a pattern reconfigurable antenna. The reconfigurable antenna is composed of four dipole elements arranged in a square shape with a microstrip line-feed. The UAV platform weighs 2.2 Kg and can sustain flight for 15 minutes. SNR measurements are conducted in various indoor and outdoor flight scenarios. Based on the experimental outcomes, it is determined that the system incorporating pattern reconfigurable antenna outperforms omnidirectional antennas in terms of achieving higher SNR in both LOS and NLOS scenarios.

I. DIRECTION OF ARRIVAL (DOA)

A compact electronically steerable parasitic array radiator (ESPAR) is designed to determine the direction of arrival (DoA) of incoming signals in WSN applications [87]. ESPAR antennas can be seamlessly incorporated into WSN nodes and gateways, addressing connectivity issues in internet of things (IoT) based systems. It is observed that existing low profile ESPAR antennas are designed for DOA estimation using the MUSIC algorithm. However, to enable received signal strength (RSS)-based DOA estimation, the ESPAR antennas must have a minimum of six distinct main beam directions. This antenna offers eight distinct main beam directions, making it suitable for cost-effective and straightforward implementation in IoT sensor nodes. Results from measurements involving power pattern cross-correlation (PPCC)-based DOA estimation suggest that the proposed design delivers overall accuracy comparable to that of a high profile ESPAR antenna with simplified beam steering and twelve distinct main beam directions. The findings demonstrate that the suggested method achieves improved accuracy in DOA estimation while reducing the overall estimation time by 33%.

J. SATELLITE AND SPACE

For low orbit vehicular satellites and aircrafts communication systems CP beam steering antennas are needed [88]. Reconfigurable antennas with multifunctional capabilities have garnered a lot of attention from the research community in the field of CubeSats. The reconfigurable antennas will be able to provide adaptability and flexibility in the compact satellite platforms [89]. A reconfigurable antenna has been developed to accommodate two distinct applications operating in different frequency bands, each with unique radiation patterns [90]. At the higher operating frequency, the antenna generates a highly directional beam with RHCP, making it suitable for vehicular satellite terminal antennas used in low-earth-orbit or medium-earth-orbit systems. On the other hand, the antenna can also support a terrestrial land mobile radio application operating at lower frequencies, providing coverage for terrestrial communication needs.

IV. PATTERN RECONFIGURABLE ANTENNAS

The pattern reconfigurable antenna designs can be classified into four categories: 1-D beam steering, 2-D beam steering, beamwidth reconfigurable antennas, and combined beam steering and beamwidth reconfigurable antennas [91]. The 1-D beam steering antennas achieves the pattern reconfiguration either in elevation or azimuth plane. Several antenna designs are reported to achieve pattern reconfiguration in a single plane based on metamaterial [92], leaky wave antenna (LWA) [93], ferrite loaded patch [94], partially reflective surface (PRS) [95], and tunable parasitic elements [4], [59], [88], [96], [97].

To enhance the radiation competence and improve the coverage, pattern reconfigurable antennas with 2-D (azimuth and elevation) beam steering capabilities are proposed in the literature. A 2-D beam steering is achieved by various techniques such as patch-slot-ring structure [98], LWA array [99], electrically tunable impedance surface [100], FSS [101], parasitic antenna design [80], [102], [103], [104], [105], [106], [107], [108], [109], [110], [111], [112], [113], [114], [115], [116], Fabry-Perot antenna [117], antenna with metamaterial slab [118], Substrate Integrated Waveguide (SIW) [119], and Complementary Split Ring Resonator (CSRR) [120]. A comprehensive performance comparison of 2-D beam steering pattern reconfigurable antennas is provided in Table 2, highlighting various aspects of their performance. It is noted that the designs reported in [98], [102], [103], [104], [108], [111], and [113] are unable to cover the complete horizontal plane. Antenna designs presented in [106] and [107] has the advantage of achieving complete azimuthal beam scanning. However, in [106], priority is given to SNR rather than to maintaining low return loss. It would be challenging to integrate this antenna into a larger array considering poor impedance matching. Also, in [107] complex biasing circuit is required to achieve desired reactance values.

The ability of wireless networks to cover more ground and handle more data can be improved by the use of beamwidth reconfigurable antennas [121]. The reported beamwidth reconfigurable antennas are based on magnetoelectric dipole [121], [122], [123], [124], [125], [126], PRS [127], [128], [129], parasitic elements [130], [131], [132], array [133], [134], [135], slotted patch [136], FSS [137], dipole [138], and switch loaded octagonal parasitic ring [139]. Table 3 provides a comprehensive comparison of beamwidth reconfigurable antennas. It is observed that the reported beamwidth reconfigurable antennas exhibit outstanding performance in terms of operating bandwidth and variability in beamwidth. It is challenging to design a beamwidth reconfigurable antenna with wide operating bandwidth, wide tunable beamwidth, and beamwidth reconfiguration in both the principal planes. Achieving beamwidth reconfigurability while incorporating polarization diversity is also a challenging task.

The majority of beamwidth reconfigurable antenna designs exhibit unidirectional radiation characteristics. There are few antenna designs that have been reported in the literature capable of attaining beam steering and beamwidth reconfigurability in a single antenna structure [81], [91], [140], [141], [142], [143], [144], [145], [146], [147]. Recently, artificially constructed metamaterial have generated a lot of interest because of their potential uses across a wide frequency band from radio waves to visible light [148], [149], [150], [151], [152]. Compared to conventional 3-D metamaterial, metasurface is a standard 2-D ultrathin planar structure consisting of sub wavelength unit structures arranged in a quasi-periodic pattern. An active integrated metasurface antenna is proposed in [145] to realize the beam steering and beamwidth reconfiguration in the operating range from 2.2 GHz to 2.7 GHz. This antenna realizes beamwidth tuning from 111° to 32° and the main beam of the antenna is steered from −39° to 36° in the E-plane. Beamwidth reconfigurability is obtained by controlling the switching conditions of the two low noise amplifiers. Switchable phase shifters cascaded with the amplifiers are used to realize beam steering.

The concept of digital coding metamaterials or programmable metamaterials is proposed in [153]. A 7 × 7 transmissive coding metasurface is used in [146] to achieve improved beam steering and beamwidth reconfigurability. The source antenna consists of an one driven element and two parasitic elements to obtain the wide beamwidth in the H-plane. By controlling the switching conditions of the PIN diodes used in the unit cell, transmission properties can be controlled. The antenna realizes discrete beam steering from −85° to 85°. The overall half-power beamwidth of the antenna can be controlled in wide and narrow beam modes. The half-power beamwidth of antenna can be discretely switched from 130° to 53°. The antenna has advantage of realizing wide beam steering along with beamwidth reconfiguration, lower side lobe level, and less gain variation. However, the antenna achieves narrow bandwidth for all the operating modes. A circular patch antenna with a vertical slot is proposed in [147] to realize reconfigurable patterns in the azimuth plane. The 3-dB beamwidth in the elevation (azimuth) plane is switchable from 82° (181°) to 190° (91°). A comprehensive analysis of beam steering and beamwidth reconfigurable antenna systems is presented in Table 4. It can be noted that designing a wideband reconfigurable antenna that can achieve beam steering and beamwidth variability within a single antenna structure is a challenging task. The wideband slot antennas can be integrated with the artificial magnetic conductors (AMCs) and coding metasurfaces to design wideband pattern reconfigurable antennas [154].

V. POLARIZATION RECONFIGURABLE ANTENNAS

In recent years, advancements in wireless communication has driven the development of polarization reconfigurable antennas that are low profile, cost-effective, and easily integrable. These antennas play a crucial role in various applications, including WLAN, read/write microwave tagging systems, satellite communication systems, etc. [19]. This section

TABLE 2. Performance evaluation of 2-D beam steering pattern reconfigurable antenna designs.

Ref.	Antenna type	Operating frequency (GHz)	Azimuth plane coverage (degree)	Main beam elevation plane (degree)	−10 dB BW (%)	Peak gain (dBi)	Substrate (dielectric constant)	Size (λ_0^3) (mm^3)	Switches (number)	Steering type
[98]	Patch-slot-ring	2.05	E & H	±22	2.6	4.58	FR4 (4.3)	1.19×1.16×0.05	PIN (4)	discrete
[103]	ESPAR	NA	$\phi = 0$ $\phi = 90$	±30 ±20	NA	NA	Rogers (3.55)	NA	varactor (2)	continuous
[104]	Cavity-backed slot ESPAR	4.1	$\phi = 0$ $\phi = 90$	−24 to 24 −20 to 20	NA	NA	Rogers (6.15)	NA	varactor (4)	continuous
[102]	Parasitic	2.5	$\phi = 0, 45, 90$	0 to 32	NA	8.51	Rogers (3)	1.25×1.25×0.027	varactor (2)	continuous
[108]	Parasitic	2.38	$\phi = 0, 45, 135, 225, 315$	0, 13, 15, 10, 12	1.68	8.2	Taconic (2.2)	1.03×1.03×0.012	PIN (4)	discrete
[111]	PIN controlled stubs	2.45	$\phi = 0, 90, 180, 270$	35	4.88	5	FR4 (4.6)	0.41×0.41×0.052	PIN (4)	discrete
[113]	Switchable director/ reflector	1.88	$\phi = 0, 45, 135, 180$	NA	34	3.7	FR4 (4.5)	0.23×0.30×0.01	PIN (4)	discrete
[80]	Parasitic pixel layer	2.45	360	30	4.08	6.5	Rogers (3.55)	0.74×0.8×0.104	PIN (12)	discrete
[107]	Reactively loaded parasitic	5	360	40	4	9.4	PTFE (2.02)	1.6×1.6×0.039	reactive loading	continuous
[109]	Parasitic	2.38	360	25	1.26	8.01	Taconic (2.2)	0.952×0.952×0.013	PIN (4)	discrete
[110]	Parasitic elements	5.5	360	30	14.5	10	Rogers (2.33)	45.2 (diameter) 3.82 (thickness)	PIN (2)	discrete
[112]	PIN controlled strips	2.4	360	36	10.48	4.5	FR4 (4.6)	0.32×0.32×0.0512	PIN (8)	discrete
[114]	Parasitic pixel layer	5.7	360	±40	4	9.5	Rogers (3)	1.14×0.8×0.039	hardwired connections (54)	discrete
[115]	Circular patch & edge grounded sector	5.8	360	24	7	8.1	Rogers (2.33)	40 (diameter) 7.15 (thickness)	PIN (12)	discrete
[116]	Dipole with parasitic striplines	2.45	360	NA	NA	6.5	Rogers (2.2)	0.57×0.45×0.253	PIN (20)	discrete
[119]	SIW horn	5	360	22.5	26.2	10	Rogers (2.33)	37 (diameter) 3.175 (thickness)	PIN (64)	discrete
[120]	CSRR on ground plane	2.45	360	±31	2.45	7.2	$\epsilon_r = 2.5$	0.82×0.78×0.025	PIN (8)	discrete

NA : Not available

provides an overview of polarization reconfigurable antennas that can provide multiple LPs [155], [156], [157], [158], [159], multiple CPs [160], [161], [162], [163], [164], [165], [166], and combinations of both [167], [168], [169], [170], [171], [172], [173], [174], [175], [176].

A. LINEARLY POLARIZED RECONFIGURABLE ANTENNAS

Linearly polarized antennas offer advantages such as cost-effectiveness and improved cross-polarization isolation. However, it is crucial to tailor polarization to the specific longitude and latitude of the deployment location. This section explores research papers that concentrate on reconfigurable antennas capable of achieving multiple LPs within a single antenna structure. The reported antenna designs are based on a dipole antenna [155], liquid metal [156], switchable feed network [157], dipole with trapezoidal-shaped arms [158], and cylindrical DRA [159].

In [155], a multi-polarization reconfigurable antenna comprising four dipoles is introduced for biomedical applications. This dipole antenna is designed to offer LPs at

TABLE 3. Performance comparison of beamwidth reconfigurable antenna designs.

Ref.	Antenna type	Operating frequency (GHz)	−10 dB BW (%)	3-dB beamwidth (degree)	Plane	Peak gain (dBi)	Switches (Number)	Beamwidth variability	Polarization
[122]	ME dipole	1.9	15	37 to 136	H	9.8	switch (2)	discrete	linear
[123]	ME dipole	2	10	80 to 160 (LP) 72 to 133 (Dual LP)	H	7.1	varactor (2)	continuous	dual linear
[124]	ME dipole	1.9	40	81 to 153	H	6.4	PIN (15)	discrete	linear
[125]	ME dipole	2.7	78.4	22 to 100 24 to 97	E H	11.5	switch (2)	discrete	dual linear
[126]	ME dipole	2.05	4.87	65 to 120 80 to 120 65 to 130	E H E, H	5.8	varactor (4)	continuous	linear
[127]	PRS	2	8	25 to 83	E	6.3	PIN (68)	discrete	NA
[128]	PRS	2	5	21 to 29.5 24 to 37	E H	15.1	varactor (100)	continuous	linear
[129]	PRS	11.2	NA	16 to 34 16 to 39	E H	NA	MEMS	discrete	dual linear
[131]	Tunable parasitic	2.475	2	50 to 112	H	8.6	varactor (2)	continuous	linear
[132]	Tunable parasitic	2.4	NA	50 to 141 53.8 to 149	E H	NA	varactor (4)	continuous	linear
[133]	Array	2.4	NA	65 to 100	H	7.36	copper strips (2)	discrete	linear
[134]	Slot antenna array	2.4	2.5 5.8 10.8	15, 31 20, 45 35, 65	E, H	14.5 12.1 7	varactor (1)	continuous	linear
[135]	Array	0.915	NA	24.1, 66.2	H	11.3	PIN (4)	discrete	NA
[136]	Slotted patch	2.3	16.24	130, 55	H	5.3, 8.6	PIN (6)	discrete	linear
[137]	FSS	5.5	NA	13.2 to 31.1	E	19	varactor (96)	continuous	NA
[138]	Dipole	2.6	4.8	77.6, 90.7, 168.3	E	NA	PIN (4)	discrete	NA
[139]	Parasitic ring	2.492	19.6	107.40 to 113.51 (ON) 74 to 77.55 (OFF)	all elevation planes	6.46	PIN (8)	discrete	circular

NA : Not available

0°, +45°, 90°, and −45°, addressing challenges related to polarization mismatch and mitigating multipath distortion in complex wireless communication systems. A polarization reconfigurable glass DRA using liquid metal is presented in [156]. The liquid metal-based reconfigurable DRA holds potential applications in wireless detection systems, where diverse types of information can be transmitted on separate channels with varying polarizations. This antenna is capable of achieving three distinct polarizations: −45°, +45°, and *y*-axis polarization. An orbital angular momentum (OAM) antenna with mode reconfigurability and polarization agility is proposed in [157]. The antenna design employs a four element uniform circular array coupled with a phase-shifting reconfigurable feed network. By controlling operating states of the PIN diodes, polarization of the resultant array can be switched between LHP or LVP. In [158], a novel wideband low-profile antenna with switchable LPs is presented. The antenna design incorporates an odd number of dipoles with trapezoidal-shaped arms printed on both sides of the substrate. These trapezoidal-shaped arms serve as reconfigurable radiators, resulting in a significantly reduced polarization interval compared to using an adjacent even number of dipoles. To achieve polarization reconfiguration PIN diodes with simple dc biasing lines are integrated. Remarkably, this antenna attains switchable seven LPs with a polarization interval of only 25.70° while maintaining an overlapped bandwidth of 17.6%. In [159], $TE_{011+\delta}$ mode is used to excite a compact horizontally polarized omnidirectional cylindrical DRA. It uses a planar feed consisting of a cross-shaped feed line, four coupled strips, and four curved arms with end-shorted stubs. The LHP and LVP can be achieved by switching between the $TE_{011+\delta}$ and $TM_{01\delta}$ modes.

B. CIRCULARLY POLARIZED RECONFIGURABLE ANTENNAS

A CP wave is characterized by the electric field vector at a given point in space tracing a circular pattern over time. The advantage of CP antennas lies in their ability to maintain effective communication even when the transmitting and receiving antennas are not perfectly aligned. This quality makes CP antennas highly practical and widely utilized in global navigation satellite systems (GNSS), including

TABLE 4. Performance comparison of reconfigurable antenna designs capable of providing beam steering and beamwidth reconfigurability.

Ref.	Antenna type	Operating frequency (GHz)	−10 dB BW (%)	360° azimuth coverage	Beam steering (degree)	3-dB beamwidth (degree)	Peak gain (dBi)	Size (λ_0^3) (mm^3)	Switches (number)
[81]	Parasitic pixel	5	4	yes	±40	40 (E-plane), 100 (H-plane) 100 (D-plane)	8	1×1×0.18	PIN (6)
[91]	Tunable parasitic	2.45	1.63	yes	10.8 (E-plane) 40 (H-plane) 32.4 (D-plane)	65 to 152 (E-plane) 64 to 116 (H-plane)	3.78	1.143×1.143×0.013	varactor (8)
[140]	PRS	2	3	no	±10 (H-plane)	18.7 to 22.4 (H-plane)	14.7	NA	varactor (100)
[141]	Antenna with metal walls	3.7	10.8	no	−51, 54 (E-plane) −20, 20 (H-plane)	narrow wide	6	0.53×0.53×0.235	PIN (2)
[142]	Tunable parasitic	1.4	6.40	no	±20 (H-plane)	60 to 130 (H-plane)	8.8	1.49×0.47×na	varactor (2)
[143]	Parasitic	3.5	5.56	no	−17, 14	49, 105	7	1.16×1.16×0.079	PIN (8)
[144]	Metasurface	3.33	NA	no	−49 to 50 (E-plane)	48, 37 (E-plane)	18	4.26×0.335×NA	varactor (90)
[145]	Metasurface	2.4	> 20	no	−39, 0, 36 (E-plane)	111 to 32 (E-plane)	14.5	1.92×1.6×0.296	two low noise amplifiers
[146]	Metasurface	3.9	0.7	no	±85	wide beam (130) narrow beam (53)	5.73	1.46×1.46×0.146	PIN (42)
[147]	Circular patch	2.08	1	yes	four steerable beams	82 to 190 (Elevation)	3	Radius 30 mm	-

NA : Not available

GPS, BeiDou system (BDS), Galileo system, and GLONASS system [16]. In this section, reconfigurable antenna designs achieving CP reconfigurability are discussed. The reported antenna designs employ various techniques, including the utilization of an E-shaped patch [160], L-shaped feeding probes [161], a combination of dipole and loop radiator [162], a switchable feed network [163], a switchable polarizer [164], liquid dielectric [165], and metasurface [166].

A polarization reconfigurable antenna presented in [160] achieves wideband characteristics with LHCP and RHCP. This antenna consists of an E-shaped patch loaded with two PIN diodes. The LHCP and RHCP operating states are produced by controlling slot lengths of the E-shaped patch. This antenna exhibits 7% effective bandwidth with a peak gain of 8.7 dBic. A L-probe fed square patch antenna with reconfigurable feeding network is used in [161] to achieve switching between LHCP and RHCP. The phase difference between two functioning L-probes can be altered between clockwise and counter clockwise by adjusting on and off states of the PIN diodes in the feeding network. A polarization reconfigurable omnidirectional antenna comprising a dipole and a loop radiator is proposed in [162]. This antenna operates at 1.575 GHz, making it suitable for use in GPS. The polarization switching between LHCP and RHCP is realized by combining three substrates, two metal probes, 48 PIN diodes, six metal pins, two capacitors, and two resistors. A dual band CP reconfigurable slot antenna is presented in [163]. The antennas far-field polarization can be altered between LHCP and RHCP by changing switching states of four PIN diodes placed in the arms of feed line.

A polarization reconfigurable CP antenna with a switchable polarizer loaded with PIN diodes is presented in [164]. This antenna employs an electrically polarization reconfigurable polarizer (EPRP) to achieve polarization reconfiguration. The LP waves radiated by the slot can be transformed into either RHCP or LHCP waves by altering operating states of PIN diodes on the polarizer. The polarizer is made up of sixteen unit cells that are stacked in a 4 × 4 array. Activating PIN diodes on the top side of the polarizer produces RHCP waves, while activating the PIN diodes on the bottom side generates LHCP waves. A CP reconfigurable patch antenna based on a fluidic control approach is presented in [165]. The antenna achieves CP radiation by exciting two orthogonal fundamental TM modes with a 90° phase difference. Polarization of this antenna can be switched between LHCP and RHCP by injecting liquid dielectric into various channels within the substrate. A low profile CP antenna with wideband and polarization reconfigurable properties is presented in [166]. This antenna comprises of a corner truncated patch and non-uniform metasurface. The non-uniform metasurface is used to generate additional operating bands in the higher frequency range. These bands are coupled with the lower band of the driven patch, resulting in a significantly broadened overall operational bandwidth.

C. LINEARLY AND CIRCULARLY POLARIZED RECONFIGURABLE ANTENNAS

In this section, the polarization reconfigurable antennas able to achieve LP as well as CP reconfigurability are discussed. Techniques used to achieve independent LP and CP reconfigurability are based on U-slot patch [167], switchable slots [168], [169], switchable feed network [171], metasurface [172], utilizing multiple resonances [174], gap-coupled patches [175], and phase change material [176].

In [167], a compact U-slot microstrip patch antenna with a switchable polarization is presented. Length of the U-slot arms can be adjusted using two beam-lead PIN diodes embedded in the slot at specific locations. By controlling operating states of the PIN diodes the U-slot becomes either symmetrical or asymmetrical enabling the patch antenna to switch between LP and CP states. In [168], a novel microstrip antenna with an X-shaped slot in the center of a rectangular patch offers polarization reconfigurability. The antenna can switch between LHP, LVP, and RHCP by adjusting geometry of the slot through the bias voltage of two PIN diodes. The antenna design in [169] features a ground plane with stair-shaped slots loaded with PIN diodes generating LP, LHCP, and RHCP states with a wide impedance bandwidth. The structure is compact, easy to optimize, and employs a simple dc bias network. The stair-shaped slots excite TM_{01} and TM_{10} modes producing distinctive resonant frequencies for CP radiation. In [171], a quad-polarization reconfigurable antenna is presented with a compact and switchable feed scheme capable of generating both LP and CP waves. The antenna can switch between $-45°$ LP, $+45°$ LP, LHCP, and RHCP by varying bias voltages of the PIN diodes. In the single-fed mode, the feed structure enables the switching of output ports generating excitation for either slant $+45°$ or $-45°$ LP states. In the dual-fed mode, it operates as a switchable phase-shifting power splitter producing either LHCP or RHCP. The antenna design optimizes utilization of the switchable feed structure in different operational states. Additionally, it is designed with a more compact size, facilitating easy integration into antenna arrays.

In [172], a low-profile metasurface antenna with wide-band capability is introduced, offering quad-polarization reconfiguration. The antenna integrates a square patch, a 4×4 periodic metal plate lattice metasurface, and four switchable feeding probes connected through two SPDTs. Dynamic polarization reconfiguration between LPX, LPY, LHCP, and RHCP states is achieved by selecting suitable feeding probes. In [174], a novel design is proposed to enhance the axial ratio bandwidth (ARBW) of a single-fed, low-profile CP reconfigurable antenna. The main radiator comprises four tiny patches in a chessboard pattern and a cross slot with uneven lengths to excite three progressively orthogonal modes, achieving two CP modes. The antenna generates three polarization states: LP, LHCP, and RHCP, with a significantly increased ARBW from 1.9% to 30.1%, surpassing conventional microstrip patch antennas. In [175], a compact, low profile antenna with wideband electrically controlled polarization reconfiguration is introduced. Utilizing quadruple gap-coupled patches, the design generates two wideband degenerative orthogonal modes. The operation mechanism involves an arrow-shaped driven element loaded with four PIN diodes, allowing dynamic control of LP, LHCP, and RHCP radiations from the quadruple gap-coupled patches. Optically controlled phase change materials are utilized in [176] to develop a polarization reconfigurable antenna operating in the mm-wave domain. The incorporation of Germanium Telluride (GeTe), a phase change material, into the antenna structure enables reconfigurability in three polarizations: LP, LHCP, and RHCP. The antenna incorporates GeTe material integrated into its four corners, with excitation provided by a microstrip line. On and off states of the material are controlled by radiation from the ultreraviolet (UV) short laser pulses.

VI. MULTIFUNCTIONAL PATTERN AND POLARIZATION RECONFIGURABLE ANTENNAS

The multifunctional pattern and polarization reconfigurable antenna has a significant capability to improve the performance of wireless communication systems. These antennas have the ability to provide both spatial and polarization diversity. Pattern and polarization reconfigurable antenna have many advantages, including multifunctional capabilities, enhancement of system capacity, avoidance of multipath distortion in wireless channels, achievement of broad radiation coverage, and polarization coding [19]. Specifically, CP beam scanning antennas are well suited for space applications. These antennas can handle many issues such as mobility, adverse weather conditions, multipath distortion, and polarization rotation effects [88]. The pattern reconfiguration properties are used to classify the multifunctional pattern and polarization reconfigurable antenna designs, as shown in Fig. 6. First, reconfigurable antennas producing broadside, conical and omnidirectional radiation pattern with polarization reconfiguration are described. Later, reconfigurable antennas radiating in forward and backward directions with polarization reconfiguration are discussed. Finally, antenna designs achieving beam steering with polarization reconfiguration are discussed in detail.

A. CLASSIFICATION BASED ON DIRECTION AND SHAPE OF THE RADIATED BEAM

In this section, reconfigurable antennas realizing variation in direction and shape of the radiated beam with polarization reconfiguration are discussed. These antennas produces broadside and conical radiation in [12], [177], [178], [179], and [180], omnidirectional and broadside radiation in [30], [89], [90], [181], [182], and [183], omnidirectional in different planes in [184], [185], [186], and [187], broadside and backfire radiation in [14], [31], and [188], beams in four directions [32], and conical and pencil beam radiation in [189].

The antenna design presented in [12] achieves two complementary radiation patterns with dual orthogonal polarization.

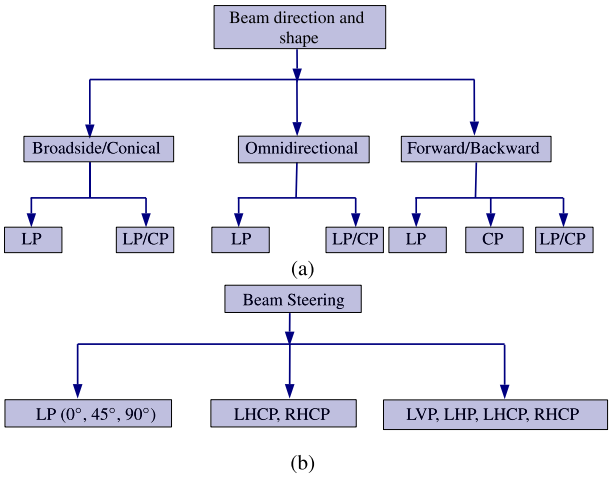

FIGURE 6. Classification of pattern and polarization reconfigurable antennas based on (a) Direction and shape of the radiated beam and (b) Beam steering.

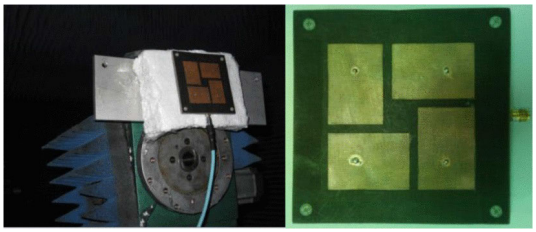

FIGURE 7. Measurement setup photograph and fabricated reconfigurable metamaterial antenna [177].

This antenna operates in two modes normal patch and monopolar patch. Antenna radiates in broadside direction with LVP and LHP. Conical radiation pattern is obtained with LPθ (linear polarization directed at an angle $\theta = 50°$). The antenna achieves overall bandwidth of 7.2%, 6.4%, and 9.4% in the LVP, LHP, and LPθ respectively. Peak gain of the antenna in broadside and conical direction is 5.5 dBi and 3 dBi respectively. A reconfigurable metamaterial antenna proposed in [177] achieves LP conical pattern and CP broadside pattern by controlling switching conditions on the feed network. This antenna achieves bandwidth of 2.1% and 41% in the LP and CP mode respectively. The 3-dB ARBW bandwidth achieved in the CP mode is 14%. The antenna exhibits a peak gain of 2.1 dBi in LP mode and 7.9 dBic in CP mode. Measurement setup photograph and fabricated reconfigurable metamaterial antenna is shown in Fig. 7.

A circular patch with shorted conductive vias are utilized in [179] to generate a broadside pattern with multiple LPs and conical beam with single LP. This antenna achieves a peak gain of 6.05 dBi for the broadside radiation pattern and 4.39 dBi for the conical radiation pattern. A 2 × 2 stacked annular ring antenna array is proposed in [180]. This antenna produces broadside radiation with ±45° and ±135° polarization. It also generates a conical radiation pattern with LVP and LHP. This antenna achieves

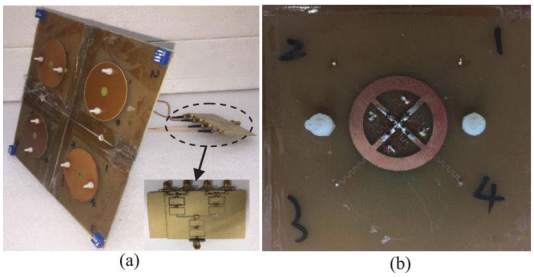

FIGURE 8. Photographs of the 2 × 2 stacked annular ring pattern and polarization reconfigurable antenna array (a) Power divider utilized to feed the array and (b) Lower patch [180].

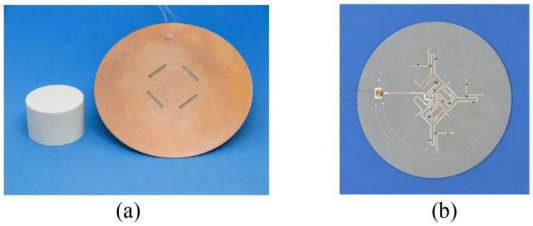

FIGURE 9. Photograph of fabricated reconfigurable DRA (a) Top view and (b) Bottom view [30].

an overall bandwidth of 13.66%. The antenna exhibits a peak gain of 12.5 dBi in the broadside direction and 6.8 dBi in the conical direction. Photographs of the 2 × 2 stacked annular ring antenna array are shown in Fig. 8.

A reconfigurable stacked square microstrip antenna proposed in [90] achieves pattern and polarization diversity at two different operating frequencies. The antenna produces high gain directional pattern with RHCP at higher frequency and low gain omnidirectional pattern with LP at lower operating frequency. However, this antenna has a large profile due to stacked design and complex structure due to dual ports. In [181], center-shorted microstrip patch is used to accomplish pattern and polarization reconfiguration. The antenna radiates in broadside direction with two orthogonal LP and produces omnidirectional radiation with LVP. The antenna exhibits an overall impedance bandwidth of 1.5%. The antenna achieves a peak gain of 6.2 dBi for the broadside radiation pattern and 3.7 dBi for the omnidirectional radiation pattern. A dielectric resonator antenna (DRA) consisting of a conventional dielectric resonator element and switchable feeding network is proposed in [30]. The antenna generates both omnidirectional and broadside radiation patterns with orthogonal LPs. Fig. 9 shows photograph of fabricated antenna.

The antenna design proposed in [182] is based on spatial-mapping origami theory, offering reconfigurable pattern and polarization for CubeSat applications. The antenna generates an omnidirectional pattern with LP and a broadside pattern with CP. The antenna design presented in [183] utilizes dielectric liquid to realize pattern and polarization reconfigurability. The polarization characteristics depend on the location of parasitic liquid DRAs. Additionally, the

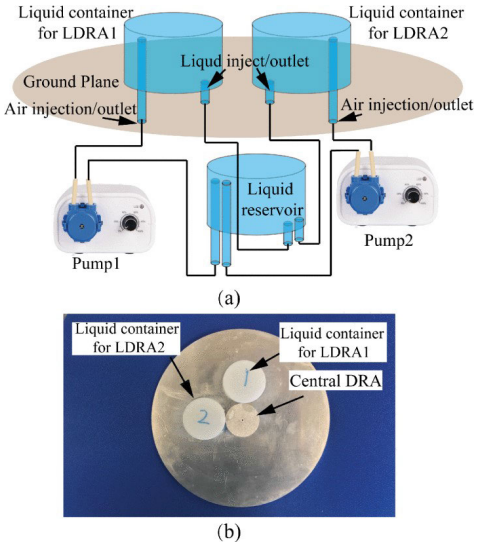

FIGURE 10. Dielectric liquid based reconfigurable antenna (a) Liquid control system and (b) Fabricated prototype [183].

radiation characteristics can be influenced by the flow of liquid, resulting in three states: omnidirectional radiation with LP, unidirectional radiation with LHP, and unidirectional radiation with LVP. Fabricated prototype of the antenna is shown in Fig. 10.

A reconfigurable antenna design based on adhesive polyimide tapes is proposed in [89] to provide reconfiguration in terms pattern, polarization, and gain level. This technique significantly reduces weight, cost, and power consumption in comparison to traditional electrical procedures that rely on active elements or complex mechanical techniques. The antenna can function both as a traditional patch antenna and as a monopole antenna. In the former configuration, it produces an omnidirectional pattern with LP in the theta direction, while in the latter configuration, it exhibits broadside radiation with LP in the Y direction.

A microstrip-fed truncated monopole antenna is proposed in [184] to achieve pattern and polarization reconfigurability. Truncated monopoles are placed next to each other on a shared ground plane and are turned on and off alternately to create omnidirectional patterns in different planes with dual orthogonal LP. The antennas compact monopole structure results in a low peak gain of −1.1 dBi. A compact coplanar waveguide (CPW)-fed reconfigurable antenna is proposed in [185] to achieve frequency, polarization, and pattern diversity. The antenna employs three switches to establish connections between four rectangular radiating patches. As the antennas polarization changes from RHCP to LHCP, the radiation pattern undergoes a rotation from 0° to 180°. A planar inverted-F antenna (PIFA) proposed in [186] achieves omnidirectional pattern in orthogonal planes with LHP and LVP. Peak gain of the antenna in LHP and LVP is 1.2 dBi and 4.2 dBi respectively. Back-to-back coupled patches fed by rat race coupler are used

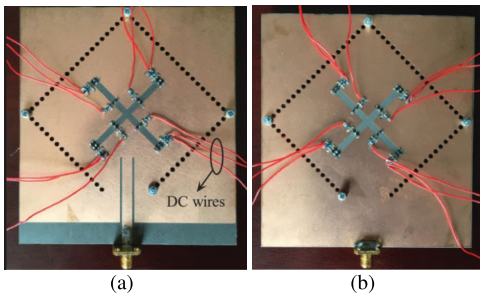

FIGURE 11. Two crossed slots loaded with switches on the SIW cavity (a) Top view and (b) Bottom view [14].

in [187] to realize pattern and polarization reconfiguration. This antenna produces omnidirectional radiation with ±45° slanted polarization. However, this antenna needs an external steering network to switch the antenna configuration. Gain of the antenna for configurations A, B, C and D varies from −0.7 to 2.7 dBi, −5.7 to 3.2 dBi, −2.4 to 2.1 dBi and −4 to 3.4 dBi respectively.

A sandwich-like reconfigurable antenna structure with two crossed slots in ground plane is presented in [188] to produce radiation in forward and backward direction with +45° and −45° slanted polarization. This work has minimal reconfigurability and fewer operating modes with similar features. In [14] compound reconfiguration is achieved by utilizing two crossed slots loaded with switches on the SIW cavity. The antennas radiation pattern can be reconfigured to either forward or backward directions with LVP, LHP, LHCP, and RHCP. For LP state, frequency of the antenna can be tuned between three states, whereas for CP mode frequency is tuned between two bands. The proposed antenna has the advantage of achieving compound reconfiguration with comparatively smaller size. Photographs of the fabricated antenna are displayed in Fig. 11.

A cuboid quadrifilar helical antenna (QHA) is presented in [31] to achieve pattern and polarization reconfiguration. The PIN diodes on radiator and feeding network are controlled to achieve orthogonal CP with radiation pattern switched between broadside and backfire. The antenna has an advantage of achieving 36.2% impedance bandwidth and 22% 3-dB ARBW. Peak gain of the antenna in broadside and backfire direction is 3.8 dBic and 4.7 dBic respectively. Photographs of the fabricated reconfigurable cuboid QHA are shown in Fig. 12. The broadside and backfire radiation patterns with polarization agility are depicted in Fig. 13.

In [32], 2 × 2 SIW ring slot antenna array is utilized to achieve pattern and polarization reconfiguration. This antenna is capable of radiating beams in four distinct directions with two orthogonal LP. A design for reconfigurable antennas based on pure water is presented in [189]. Within a specific frequency range, a rod made of pure water can function as a wave-guiding medium. It is noted that the water antennas working frequency should be below the dielectric waveguides cut-off frequency. Three pure-water

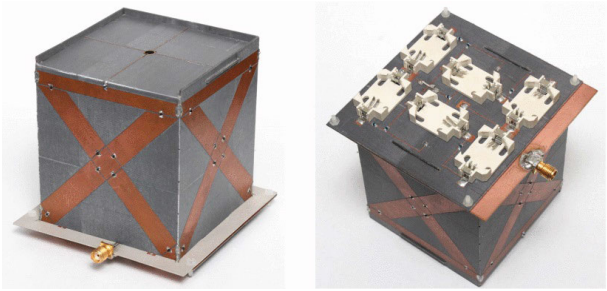

FIGURE 12. Photographs of the fabricated reconfigurable cuboid quadrifilar helical antenna (QHA) [31].

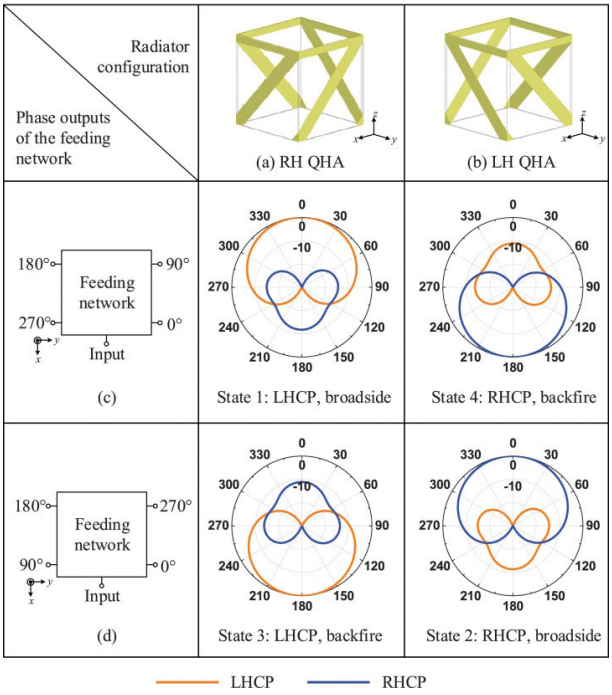

FIGURE 13. Broadside and backfire radiation patterns with LHCP and RHCP operating states [31].

rod antennas-Vee, normal-mode helix, and CP monopole has been developed. The proposed antennas produces conical and pencil beam with LP and LHCP operating states. Table 5 summarizes detailed results for pattern and polarization reconfigurable antenna designs radiating in different directions and producing different beam shapes.

B. BEAM STEERING WITH LINEAR POLARIZATION RECONFIGURATION

In this section, the multifunctional pattern and polarization reconfigurable antennas achieving pattern reconfiguration in terms of beam steering with LP reconfiguration are discussed in detail. Techniques used to achieve beam steering with polarization reconfiguration are presented in Fig. 14.

The beam steering with LP reconfiguration is achieved by various techniques such as tunable parasitic elements [42], [190], [191], PRS [192], and liquid-metal [72]. The utilization of tunable parasitic elements and reconfigurable feeding network enables the realization of beam steering with multiple LPs [42]. Fabricated prototype of the antenna is shown in Fig. 15. This antenna achieves three different LPs in $\phi = 0°$, $45°$, and $90°$ planes. For each polarization state the antenna is capable of radiating in the horizontal plane (H-plane) at angles $20°$, $0°$ and $-20°$, as depicted in Fig. 16.

A cross patch antenna with one driven element and four parasitic elements is presented in [190]. The main beam direction is altered by employing a shorting switch that connects the radiating element to the ground plane. This antenna radiates in six different directions in the azimuth and elevation plane with LHP or LVP. Polarization reconfiguration is accomplished by exciting driven element with two separate feeds. This antenna works according to microstrip Yagi principle with parasitic elements can be used as director or reflector.

In [191], a pattern and polarization reconfigurable antenna is introduced, capable of generating two distinct LPs and one diagonal polarization. This antenna employs PIN diodes on parasitic elements whose bias voltage can be adjusted, enabling the antenna to produce five different beams in each polarization state. Fig. 17 illustrates the prototype fabrication of this antenna, which features reconfigurable parasitic elements comprising printed dipoles with PIN diodes positioned between their halves. These PIN diodes control the operating states of the parasitic elements, allowing them to function as directors or reflectors. Moreover, a reconfigurable feeding network is utilized to achieve polarization reconfiguration, allowing two orthogonal polarizations and one diagonal polarization. Main beam of the antenna is directed at a $45°$ angle in the elevation plane across all three beams (beam 1, beam 2, and beam 3), as depicted in the Fig. 18. Furthermore, the radiation pattern of beam 4 and beam 5 in the $\phi = 45°$ plane is presented in Fig. 19.

A Fabry-Perot cavity antenna with a reconfigurable PRS is proposed in [192] to achieve 2-D beam steering with LP. The LVP and LHP are achieved through the utilization of an aperture-coupled patch antenna. Additionally, the pattern reconfiguration is accomplished by controlling the reflection phase distribution of PRS using PIN diodes. An electrically actuated liquid-metal reconfigurable dipole antenna is presented in [72]. It provides null steering with five discrete LPs, $0°$, $\pm 45°$ and $\pm 90°$. Detailed results of the antenna deigns achieving beam steering with LP reconfiguration are summarized in Table 6.

C. BEAM STEERING WITH CIRCULAR POLARIZATION RECONFIGURATION

It is observed that most of the pattern reconfigurable antenna designs reported in the literature are linearly polarized. Pattern reconfiguration with CP is a difficult task to accomplish and is found to be very limited in the literature. Wireless communication applications need reconfigurable antenna capable of radiating waves in more than one steering angle with polarization agility. Techniques used to realize CP beam switching, as shown in Fig. 20 are based on

TABLE 5. Performance comparison of antenna designs achieving variation in direction and shape of the radiated beam with polarization reconfiguration.

Ref.	Antenna type	Operating frequency (GHz)	Radiation pattern	Polarization	−10 dB BW (%)	3-dB AR BW (%)	Peak gain	Size (λ_0^3) (mm^3)	Switches (number)
[12]	Square-ring patch	2.44	broadside conical	LVP, LHP LPθ	7.2, 6.4 9.4	- 	5.5 3	0.81×0.81×0.0048	PIN (4)
[177]	Metamaterial	2	conical broadside	LP CP	2.1 41	- 14	2.1 7.9	0.66×0.66×0.033	copper strips (12)
[179]	Circular patch with vias	2.45	broadside conical	multiple LP single polarization	2.5	-	6.05 4.39	80 (diameter) 1.52 (thickness)	PIN (16)
[180]	2×2 stacked annular ring array	2.4	broadside conical	±45, ±135 HP, VP	13.66	-	12.5 6.8	1.6×1.6×0.056	PIN (16)
[90]	Stacked square antenna	0.67 1.75	omnidirectional broadside	LP RHCP	7.3 15.8	- 10	3.9 7.5	0.76×0.76×0.058	PIN (3)
[181]	Center shorted microstrip patch	3.67	broadside omnidirectional	LP (ϕ = 0 & 90) VP	1.5	-	6.2 3.7	NA	PIN (12)
[30]	DRA	2.45	omnidirectional broadside broadside	vertical LHP LVP	6.2 8.2 7.4	-	2.5 4.9 5.0	1.05×1.05×0.25	PIN (6)
[182]	Dipole array antenna	5.8	omnidirectional broadside	LP CP	33	33	0.5 8.07	1.93×1.93×0.0097	mechanical
[183]	DRA	2.4	omnidirectional unidirectional unidirectional	LP LHP LVP	22.9 23 23	-	4.2 6.32 6.32	NA	NA
[89]	Adhesive polyimide tapes	2.4	Broadside Omnidirectional	LPY LPθ	2-4.1	-	7.7 1.2	1.272×1.216×0.0254	-
[184]	Microstrip truncated monopole	2.4	omnidirectional in different planes	LVP LHP	4.1	- -	−1.1	0.152×0.152×0.0128	copper strips (2)
[185]	CPW-fed monopole	5.81 5.07 5.09 5.11	omnidirectional in different planes	LP LP LHCP RHCP	22.54 23.66 44.01 33.85	- - 38.8 33.66	2.9 3.4 3.7 3.5	0.26×0.26×0.035	copper strips (3)
[186]	PIFA monopole	2.4	omnidirectional in different planes	HP VP	8.4	-	1.2 4.2	0.4×0.4×0.012	PIN (1)
[187]	coupled patches fed by coupler	2.56	omnidirectional in different planes	±45	NA	-	3.4	NA	-
[188]	Crossed slots	2.5	broadside backfire	+45 −45	NA	-	NA	0.42×0.42×0.033	PIN (8)
[14]	Cavity-backed antenna	2.29 2.31	forward, backward	LVP, LHP LHCP, RHCP	≈2 ≈3.5	- ≈2.35	4.7	1.03×0.93×0.012	PIN (48)
[31]	Cuboid quadrifilar helical antenna	0.9	broadside, backfire	LHCP, RHCP	36.2	22	3.8, 4.7	0.26×0.26×0.25	PIN (32)
[32]	SIW ring-slot 2×2 array	5.8	beams in four directions	2 orthogonal LP	2.59	-	11.6	2.54×1.27×0.095	PIN (2)
[189]	Water monopole array	2	conical beam pencil beam	LP LHCP	21.3	30.5	5.8 6.9	radius 100	-

NA : Not available

spiral [193], waveguide [194], metasurface [195], parasitic [88], LWA [196], dipole [197], RFN [198], SIW [199], transmitarray [200], reflectarray [201], DRA [202], and Fabry-Perot antenna [203]. However, it is worth noting that these reported antenna designs do not achieve polarization reconfiguration. The beam steering is accomplished using

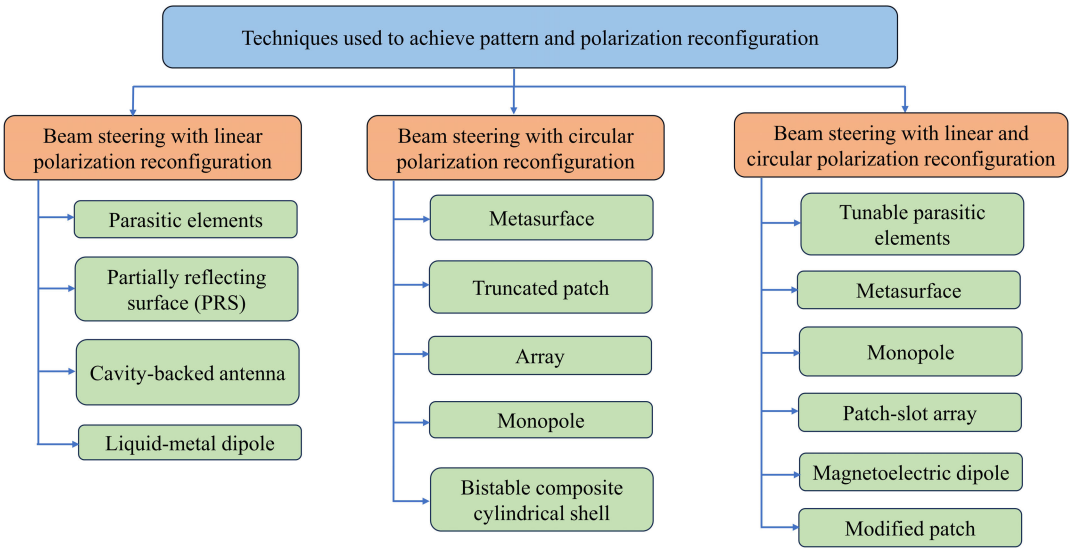

FIGURE 14. Techniques used to achieve beam steering with polarization reconfiguration.

TABLE 6. Performance comparison of pattern and polarization reconfigurable antenna designs achieving beam steering with multiple LP.

Ref.	Antenna type	Operating frequency (GHz)	360° azimuth coverage	Main beam elevation plane (degree)	Polarization	−10 dB BW (%)	Peak gain (dBi)	Size (λ_0^3) (mm^3)	Switches (number)
[42]	Cavity-backed proximity coupling	11	no	−20, 0, 20	LP 0°, 45°, 90°	NA	8.12	1.17×1.17×0.37	PIN (10)
[190]	Parasitic	10	no	3 beam patterns	HP, VP	NA	6.7	0.73×0.73×0.026	copper strips (4)
[191]	Parasitic	2.4	yes	45	LVP, LHP, diagonal LP	≈0.8	3.5	1.2×1.2×0.232	PIN (8)
[192]	PRS	5.5	yes	0, 10, −10	LVP, LHP	≈3.6	9.7	1.83×1.83×0.513	PIN (144)
[72]	Liquid-metal dipole	1.579	no	null steering	five discrete LP 0°, ±45°, ±90°	NA	2.08	0.0079×0.14×0.0032	liquid-metal

NA : Not available

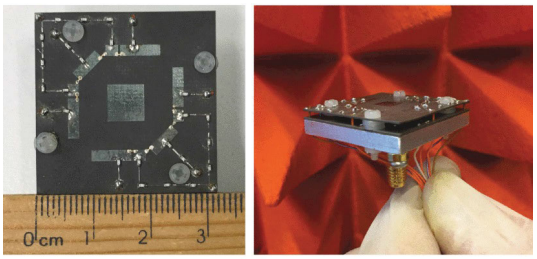

(a) (b)

FIGURE 15. Prototype of the cavity-backed reconfigurable microstrip antenna (a) Top view and (b) Overall view [42].

either LHCP or RHCP. In this section, multifunctional pattern and polarization reconfigurable antennas with the capability of realizing beam steering with multiple CP are discussed.

A pattern and polarization reconfigurable proposed in [204], consists of a metasurface and a slot antenna. The antenna is capable of discrete beam switching within a range of −20° to 20° with LHCP and RHCP. This antenna exhibits an overall impedance bandwidth of 2% and achieves a peak gain of 8 dBi. Conventionally, beamforming networks consisting of couplers and phase shifters are used to obtain 2-D switchable beams. However, these beamforming networks require a larger amount of circuit space and are frequency dependent. To address these limitations, a pattern and polarization reconfigurable antenna is developed utilizing the spatial phase technique [39]. This approach employs a 2 × 2 patch antenna array fed by switchable feeding probes to achieve independent polarization reconfiguration and beam switching. Fig. 21 illustrates the distribution of surface currents on the parasitic patch at an operating frequency of 4.8 GHz, showing various

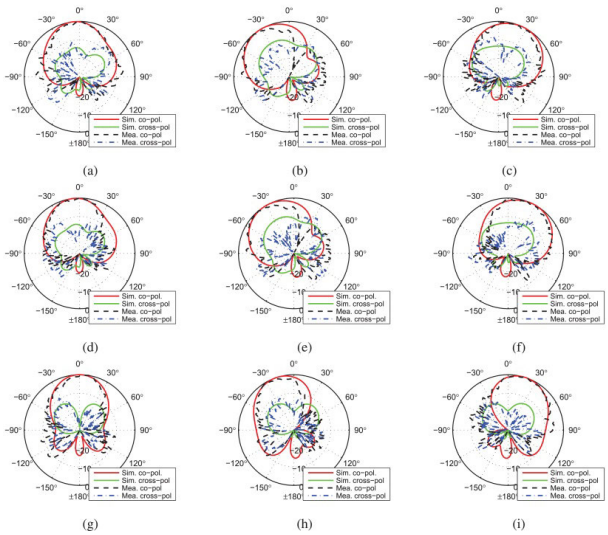

FIGURE 16. Simulated and measured H-plane radiation patterns at 11 GHz for all the nine working modes [42].

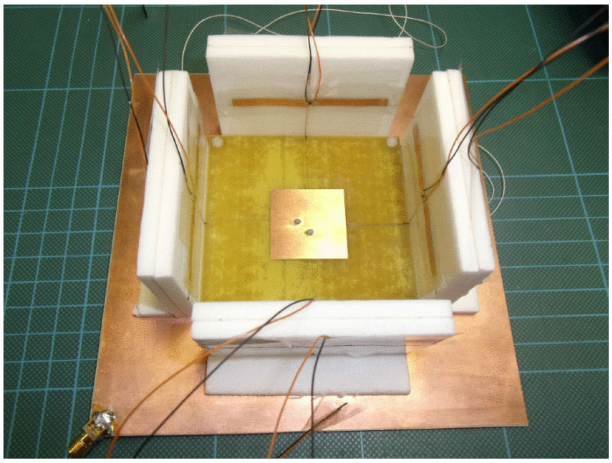

FIGURE 17. Fabricated antenna prototype realizing beam switching with LP reconfiguration [191].

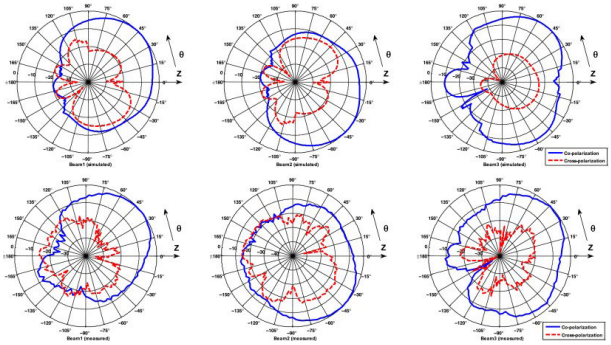

FIGURE 18. Simulated and measured radiation patterns in $\phi = 90°$ (Beams 1 and 2) plane and $\phi = 0°$ (Beam 3) plane [191].

time phases with different feeding probe excitations. The prototype fabrication is shown in Fig. 22. The radiated beam is switched to $\theta = \pm 16°, \pm 16°, \pm 28°$, and $\pm 28°$ for $\phi = 0°$,

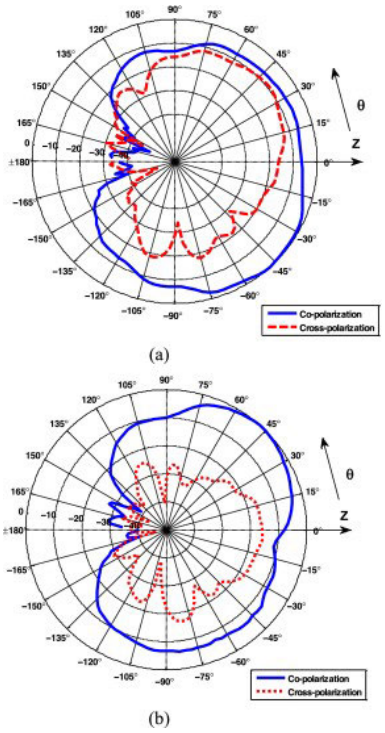

FIGURE 19. Measured radiation patterns in $\phi = 45°$ plane (a) Beam 4 and (b) Beam 5 [191].

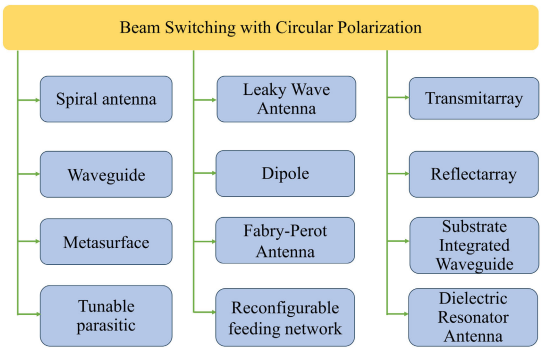

FIGURE 20. Techniques used to realize CP beam switching.

90°, 45°, and 135° respectively with LHCP and RHCP states. It is noted that the antenna is able to provide coverage across the entire azimuth plane. This antenna utilizes the spatial phase technique to improve the ARBW. It attains a peak gain of 10.5 dBi, while exhibiting an overall impedance and ARBW of 9.07%.

A novel compound reconfigurable antenna based on a monopole design is proposed in [40] for future 5G applications. The structural configuration of the monopole-based compound reconfigurable antenna is illustrated in Fig. 23. This antenna offers the ability to reconfigure its operating frequency, radiation pattern, and polarization. It operates in two frequency bands, specifically at 3.5 GHz and 5.5 GHz. Within each operating band, the antenna can switch its polarization from LHCP to RHCP with a discrete beam switching

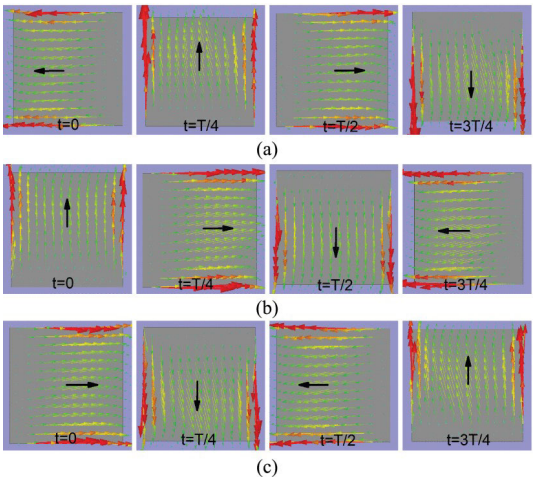

FIGURE 21. Simulated surface current distribution on the parasitic patch at an operating frequency of 4.8 GHz with (a) Excitation at probe 1, (b) Excitation at probe 2, and (c) Excitation at probe 3 [39].

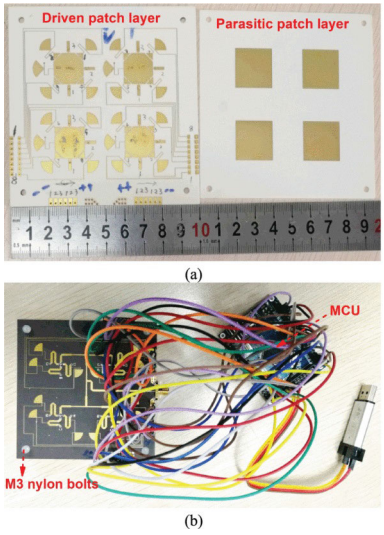

FIGURE 22. Photographs of the fabricated 2 × 2 patch antenna array (a) Driven and parasitic patch layer and (b) Bottom view of the installed array antenna with MCU [39].

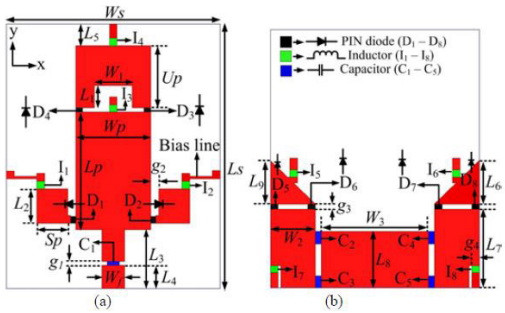

FIGURE 23. Structural configuration of the monopole-based compound reconfigurable antenna [40].

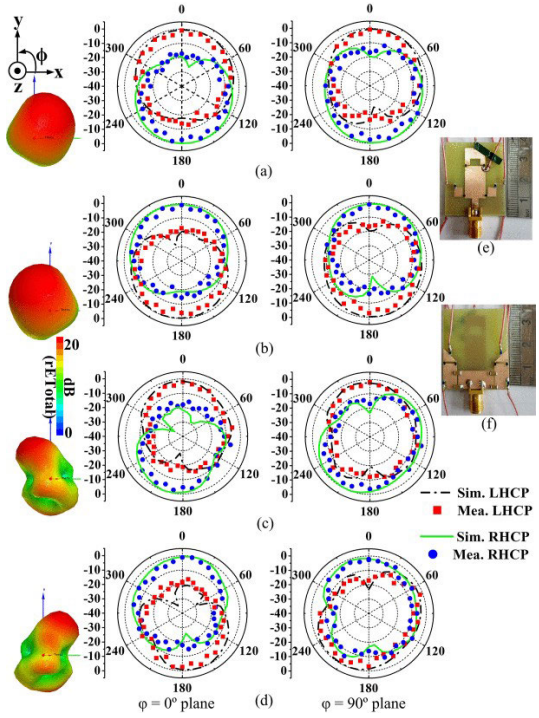

FIGURE 24. Simulated and measured normalized far-field patterns are depicted with 3-D plots for operating modes in (a) LHCP (at 3.6 GHz), (b) RHCP (at 3.6 GHz), (c) LHCP (at 5.5 GHz), (d) RHCP (at 5.5 GHz), (e) Front view of the fabricated antenna, and (f) Back view of the fabricated antenna [40].

angle of ±30°. Fig. 24 shows the normalized simulated and measured far-field radiation patterns at 3.6 GHz and 5.5 GHz, along with a photograph of the fabricated antenna.

In [20], a compound reconfigurable antenna array consisting of a 1 × 4 patch configuration is presented, offering the capability to reconfigure its frequency, radiation pattern, and polarization. The specific arrangement of the 1 × 4 compound reconfigurable antenna array is shown in Fig. 25. The antenna is able to produce five beam states with LHCP and RHCP. The pattern and polarization reconfiguration characteristics are obtained in four different frequency bands. The connection between the activated feeding probes, polarization, and radiation beam is outlined in Fig. 26.

A proposed design in [41] introduces a CP-agile and continuously beam steerable array antenna that combines digital

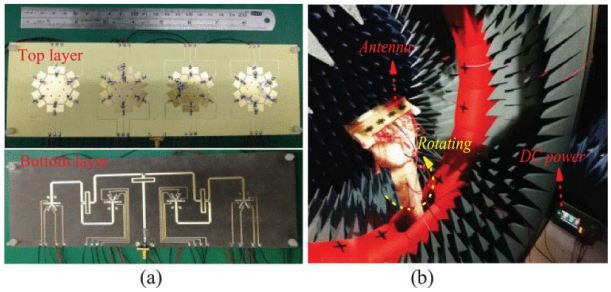

FIGURE 25. (a) Photograph of the 1 × 4 compound reconfigurable antenna array and (b) Measurement setup in the anechoic chamber [20].

reconfigurable antenna elements and analog tunable phase shifters. This hybrid approach offers several advantages, including high scanning resolution, easy implementation, and

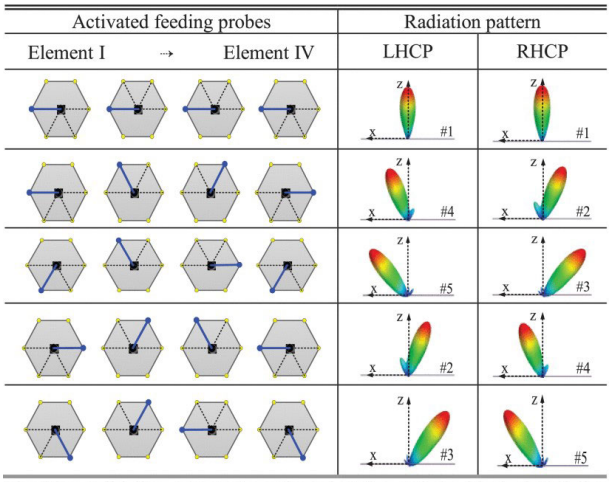

The blue solid line represents activated probe and the black dotted line represents inactivated probe.

FIGURE 26. Beam states generated by different activated feeding probes [20].

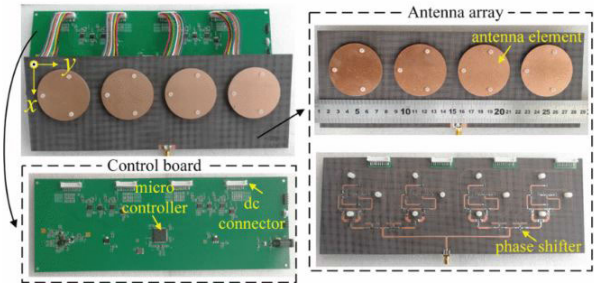

FIGURE 27. Fabricated prototype of the antenna array [41].

low cost. By manipulating the biasing states of PIN diodes and varactors, the four element array achieves a beam steering range of ±40° for both LHCP and RHCP. The antenna exhibits excellent impedance matching and CP performance within the overlapping frequency band of 2.43 to 2.63 GHz. A fabricated prototype of the array antenna, featuring digital reconfigurable antenna elements and analog tunable phase shifters, is depicted in Fig. 27.

In [205], a novel antenna design utilizing bistable composite cylindrical shells is introduced, offering wideband pattern and polarization reconfigurability. The antenna allows for the variation of polarization between LHCP and RHCP, while also enabling the adjustment of primary lobes of the radiation patterns by up to 80° in various configurations. Fig. 28 shows a fabricated prototype of the bistable reconfigurable antenna.

The utilization of LWAs for beam steering has become increasingly popular due to their advantageous characteristics such as a simple feed structure and easy fabrication. These advantages contribute to cost reduction and simplification of the overall antenna system. However, it should be mentioned that the majority of LWAs achieve beam steering primarily in the broadside direction with a fixed polarization state. The reconfigurable LWA achieves both polarization

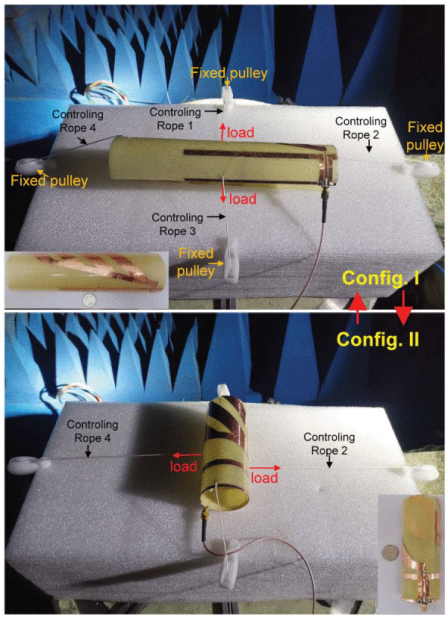

FIGURE 28. Fabricated wideband pattern and polarization reconfigurable antenna utilizing bistable composite cylindrical shells [205].

agility and continuous beam scanning capabilities [206]. The antennas polarization can be switched between LP and CP states. Furthermore, the main beam of the antenna can be continuously scanned within the LP state from −34.3° to 20°, and within the CP state from −31.5° to 17.1°. Table 7 presents performance comparison of pattern and polarization reconfigurable antenna designs achieving beam steering with CP reconfiguration. It is noted that the reported designs realize pattern reconfigurability over a limited impedance and ARBW.

D. BEAM STEERING WITH LINEAR AND CIRCULAR POLARIZATION RECONFIGURATION

This section provides an overview of antenna designs realizing pattern variability with LP as well as CP reconfiguration. The reported antenna designs are based on tunable parasitic [13], [33], [207], [208], [209], metasurface [210], planar monopole [34], rhombic patch [35], patch slot array [36], patch with metal wall [211], ME dipole array [37], reconfigurable endfire dipole-pair elements [212], and phased array [38] for realizing beam steering with both LP and CP.

In [207], the driven and four circular parasitic elements are mutually coupled to reconfigure pattern and polarization. For LP mode, the main beam is directed to broadside, 4°, and ±19°, whereas with LHCP the main beam is switched to ±10°. A reconfigurable antenna with parasitic patch layer is presented in [208], to realize discrete beam switching with LP and CP. The CP is obtained by making rectangular slits on the parasitic elements. The primary beam of the antenna can be discretely switched to −30°, 0° and 30° with both LP and CP. The prototype fabrication is shown in Fig. 29. To achieve

TABLE 7. Performance comparison of pattern and polarization reconfigurable designs achieving beam steering with CP reconfiguration.

Ref.	Antenna type	Operating frequency (GHz)	360° azimuth coverage	Main beam elevation plane (degree)	Polarization	−10 dB BW (%)	3-dB AR BW (%)	Peak gain	Size (λ_0^3) (mm^3)	Switches (number)
[204]	Metasurface	5	no	−20, 0, 20	LHCP, RHCP	2	2	8	1.3×1.3×0.0398	PIN (32)
[39]	Truncated patch	4.8	yes	broadside, ±16, ±28	LHCP, RHCP	9.07	9.07	10.5	1.6×1.6×0.074	PIN (12)
[40]	Monopole	3.5 5.5	no	+30 −30 +30 −30	LHCP RHCP LHCP RHCP	38.05 34.48 16.67 18.86	7.11 7.68 16.65 15.97	1.02 1.11 0.85 0.91	0.32×0.40×0.019	PIN (8)
[20]	1×4 array	2.18 2.4 2.68 2.95	no	±50	LHCP RHCP	32.68	NA	8	0.64×1.92×0.017	PIN (32) varactor (24)
[41]	1×4 array	2.5	no	±40	LHCP RHCP	7.9	7.9	11.1	NA	PIN (12) varactor (2)
[205]	Bistable composite cylindrical shell	2.7	no	80	LHCP RHCP	26.4	26.4	9.6	volume 612.5 cm^3	-

NA : Not available

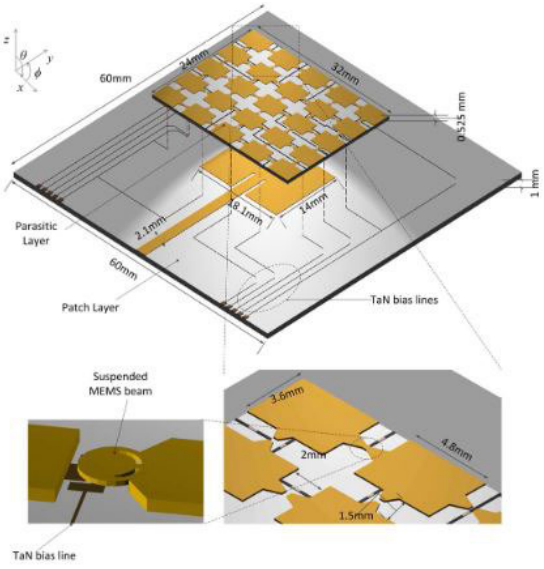

FIGURE 29. 3-D Schematic of the multifunctional reconfigurable antenna [208].

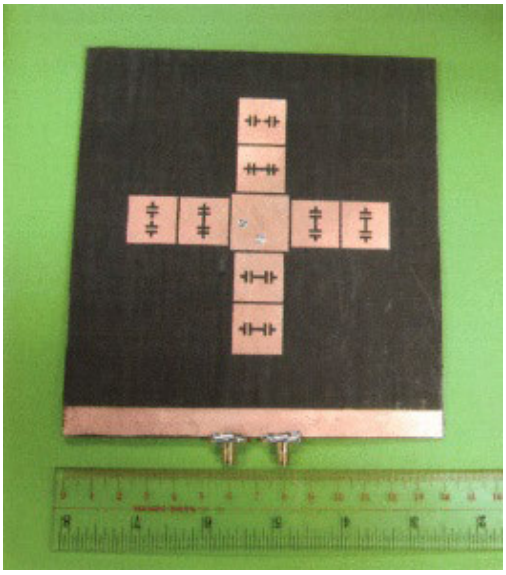

FIGURE 30. Top view of the reconfigurable crossed-Yagi patch antenna [209].

pattern diversity and polarization selectivity, a crossed Yagi patch antenna is proposed in [209]. This design includes two identical linear Yagi-Uda patch arrays that are reconfigurable and positioned orthogonally around a single driven element. The prototype fabrication of this antenna is shown in Fig. 30. In terms of performance, primary beam of the antenna is tilted approximately 35° in the elevation plane for both LP and CP configurations.

The antenna design presented in [13] incorporates a parasitic layer consisting of metallic pixels arranged in a 6×6 grid above the driven element. This arrangement enables compound reconfiguration, including changes in frequency, pattern, and polarization. The antenna supports LVP, LHP, LHCP, and RHCP. The primary beam of the antenna can be discretely switched to a ±30° angle in both the *xz*-plane and *yz*-plane. Frequency tuning between 12% and 25% is achieved by adjusting the distance between the driven and parasitic elements. The fabricated prototype of the parasitic pixel antenna is displayed in Fig. 31. The antenna design presented in [33] consists of four parasitic elements and

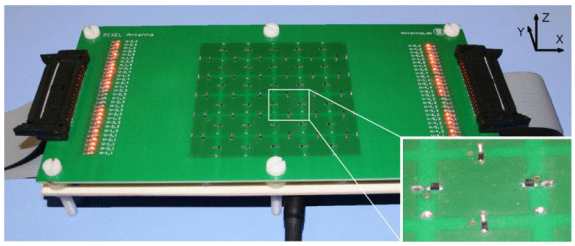

FIGURE 31. Picture of the pixel antenna prototype placed above the driven element [13].

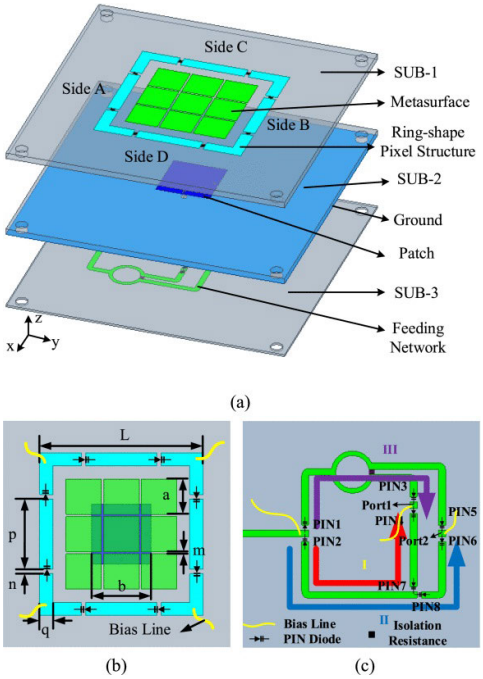

FIGURE 32. Metasurface based pattern and polarization reconfigurable antenna (a) 3-D view, (b) Top view, and (c) Bottom view [210].

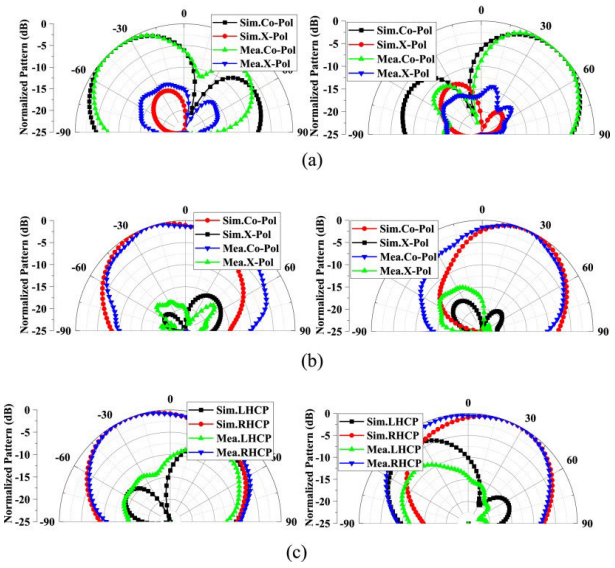

FIGURE 33. Normalized simulated and measured radiation patterns in the *yz*-plane at the center frequency of 5 GHz (a) HP, (b) VP, and (c) CP [210].

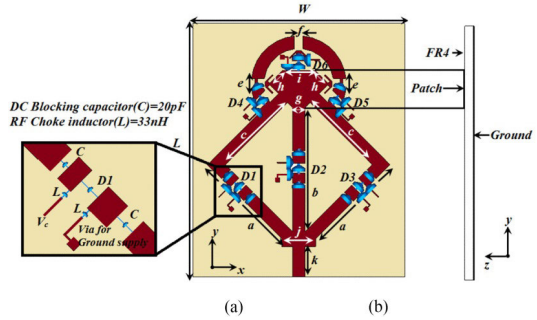

FIGURE 34. Geometry of the rhombus-shaped compound reconfigurable antenna [35].

a reconfigurable feeding network to achieve independent pattern, beamwidth, and polarization reconfiguration.

In [210], a pattern and polarization reconfigurable antenna based on a metasurface is proposed, as depicted in Fig. 32. The reconfigurable feeding network utilizes two OR circuits, a 3 dB power divider, and eight PIN diodes to achieve HP, VP, and CP operating states. Pattern reconfiguration is achieved by controlling the PIN diodes on the ring-shaped pixel structure. Main beam of the antenna is steered to $\pm 40°$ with HP, $\pm 20°$ with VP, and $\pm 25°$ with CP in the *yz*-plane, as illustrated in Fig. 33. The symmetrical structure of the antenna ensures that pattern and polarization reconfigurability can also be achieved in the *xz*-plane.

A reconfigurable loop antenna design proposed in [34] realizes pattern and polarization diversity. This antenna simultaneously changes the radiated beam in *xz*-plane and *yz*-plane with LP, LHCP, and RHCP operating states. A rhombus-shaped compound reconfigurable antenna is proposed in [35]. This antenna utilizes six pairs of BAR64-03W series PIN diodes. The time it takes for the PIN diode to switch from a forward bias to a reverse bias state is 0.095 seconds, while the transition time from a reverse bias to a forward bias state is 7 microseconds. Fig. 34 presents geometrical structure of the rhombus-shaped compound reconfigurable antenna. The antenna operates at two frequencies 5.2 and 5.8 GHz. Polarization can be switched between LP, circular, and $\pm 45°$. However, all the mentioned polarizations are not achieved at both operating frequencies; at 5.2 GHz, $\pm 45°$ slant polarization is achieved, while at 5.8 GHz, LP, LHCP, and RHCP are obtained. Fig. 35 and Fig. 36 displays both simulated and measured radiation patterns at the center frequency of 5.8 GHz.

The antenna design proposed in [36] uses truncated circular radiator, C-shaped parasitic elements and perturbed rhombic slot to realize compound reconfiguration. This antenna achieves LP at both the operating frequencies, whereas LHCP and RHCP is obtained at 3.6 GHz and 5.8 GHz respectively. Radiation pattern of the antenna can be switched to broadside, omnidirectional, and $\pm 30°$ with LP.

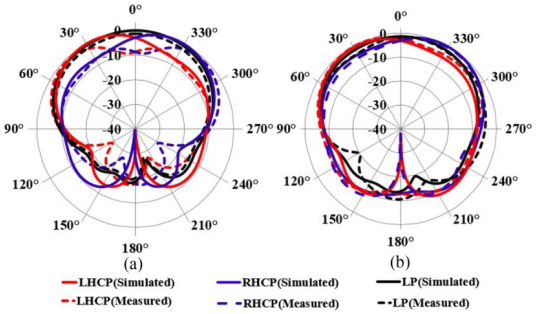

FIGURE 35. Simulated and measured radiation pattern at 5.8 GHz for LHCP, RHCP, and LP state (a) H-plane and (b) E-plane [35].

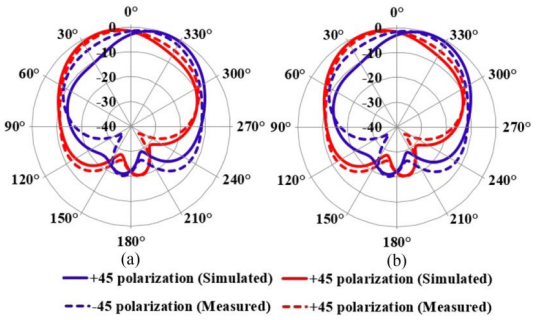

FIGURE 36. Simulated and measured radiation pattern at 5.8 GHz for ±45° slant polarization (a) H-plane and (b) E-plane [35].

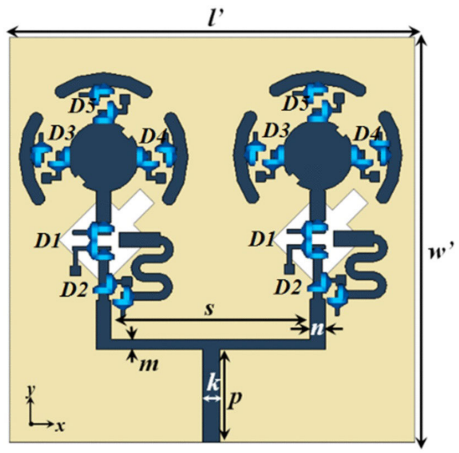

FIGURE 37. Geometry of the 1 × 2 antenna array [36].

However, with LHCP and RHCP radiation main beam of the antenna is always directed in broadside direction. Geometry of the 1 × 2 antenna array is shown in Fig. 37.

In [211], a multidirectional beam and multipolarization antenna is introduced. This antenna comprises a feed section, a radiating patch, four diagonal metal walls, and four switches. Pattern and polarization reconfigurability are achieved by connecting the metal walls to the ground plane using PIN diodes. The antenna operates in eight modes: LP patterns with narrow and wide beamwidths, LP with ±20° beam switching in the *xz*-plane and *yz*-plane, and

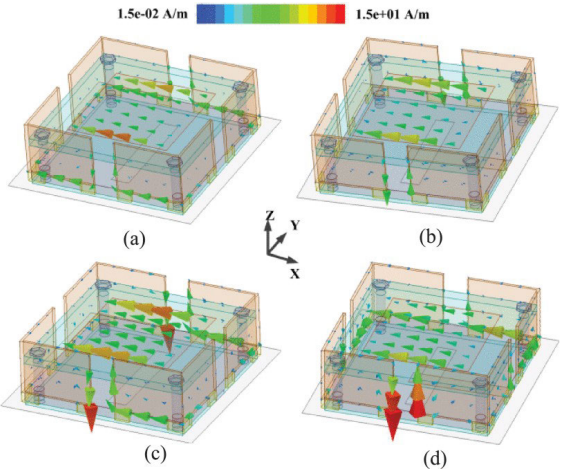

FIGURE 38. Surface current distribution of the antenna with LP in (a) Mode 1, (b) Mode 2, (c) Mode 3, and (d) Mode 5 [211].

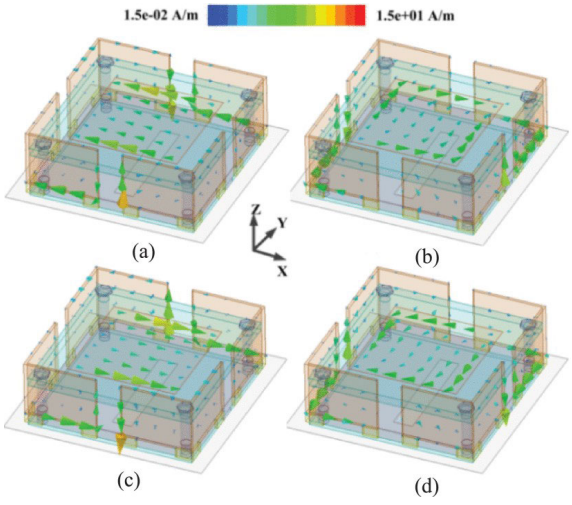

FIGURE 39. Surface current distribution of the antenna with LHCP in Mode 7 (a) t = 0, (b) t = T/4, (c) t = T/2, and (d) t = 3T/4 [211].

LHCP and RHCP with wide 3-dB beamwidth and 3-dB AR beamwidth. An advantage of this antenna is achieving a wide 3-dB AR beamwidth for LHCP and RHCP configurations. Fig. 38 illustrates surface current distribution of the antenna operating in an LP state under various modes. In mode 1, a broadside radiation pattern with a narrow beam is achieved with current distribution along the *x*-axis. Mode 2 results in a wide beamwidth pattern due to vertical current generated on the diagonal metal wall. Modes 3 and 4 steer the main beam of the antenna to +20° and −20°, respectively, in the *xz*-plane, with currents concentrated on the radiating patch and diagonal metal walls. Similarly, modes 5 and 6 achieve beam steering of ±20° in the *yz*-plane. Fig. 39 presents surface current distribution of the antenna in LHCP state for mode 7, radiating LHCP pattern with wide beamwidth. In mode 8, RHCP is obtained with wide beamwidth.

A pattern and polarization reconfigurable antenna comprising of cavity-backed 1 × 4 ME dipole antenna array is

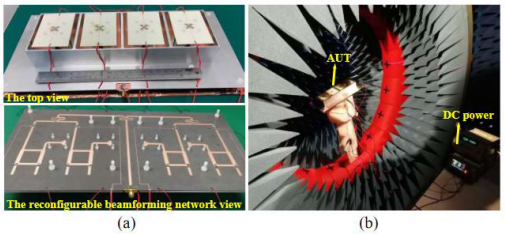

FIGURE 40. (a) Photograph of the assembled 1 × 4 cavity-backed ME dipole antenna array and (b) Measurement environment in the anechoic chamber [37].

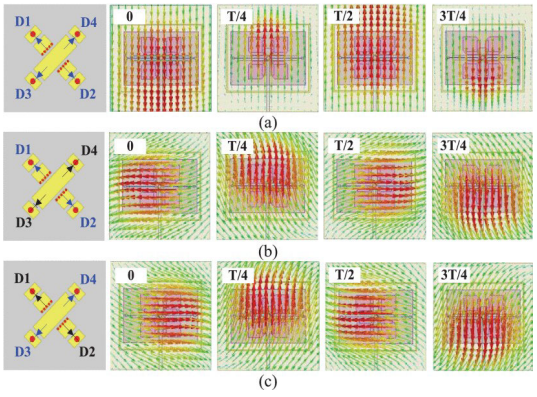

FIGURE 41. Simulated electric field distribution in (a) LP, (b) LHCP, and (c) RHCP state [37].

presented in [37]. The antenna is able to realize continuous beam scanning of ±40° for the three different polarization states LP, LHCP, and RHCP. The pattern reconfiguration is achieved by reflection-type phase shifters loaded with the varactor diodes. In all the operating modes, antenna maintains the −10 dB impedance and 3-dB ARBW in the range of 2 to 2.4 GHz. Fig. 40 shows photograph of the 1 × 4 antenna array. Two switchable cross strips are embedded into the ME dipole element to realize polarization reconfiguration. Fig. 41 shows the simulated current distribution on the two switchable cross strips at an operating frequency of 2.25 GHz. When both cross strips are activated, the antenna operates in LP state, while activating one strip produces CP state. For instance, with D1 and D2 ON and D3 and D4 OFF, LHCP mode is achieved, whereas switching D1 and D2 OFF and D3 and D4 ON results in RHCP mode. Thus, by controlling state of the switchable cross strips, the antennas polarization can be switched among LP, LHCP, and RHCP modes. The normalized simulated and measured radiation patterns for all the operating modes are depicted in Fig. 42.

A 3-D pattern reconfigurable antenna array with multi-polarization is presented in [212]. This antenna achieves five independently controlled polarizations with twelve different radiation patterns. Fig. 43 shows photograph of the fabricated prototype. A 1 × 4 phased array consisting of circular patch with an annular microstrip ring is presented in [38]. Four varactor diodes are loaded on the ring to achieve frequency tuning from 1.5 to 2.4 GHz. RFN is used to obtain two orthogonal LP and CP. The antenna achieves beam steering of ±28° at 2.4 GHz and ±52° at 1.5 GHz. Geometry of the antenna array is shown in Fig. 44. Table 8 summarizes results of antenna designs which achieves beam steering along with the polarization reconfiguration.

VII. PERFORMANCE COMPARISON

This section provides a performance evaluation of the multifunctional pattern and polarization reconfigurable antennas that have been discussed. Table 5 provides a comprehensive overview of specific outcomes for antenna designs that offer reconfigurable patterns and polarizations, radiating in various directions and generating diverse beam configurations. A limitation observed in the presented antenna designs [12], [14], [31], [32], [90], [177], [179], [180], [181], [184], [185], [186], [187], [188] is that the reconfiguration of pattern and polarization cannot be achieved independently. The pattern and polarization characteristics of these antennas are linked to the geometrical design and arrangement of the antenna elements. In practical applications, reconfigurable antenna designs achieving independent reconfiguration antenna parameters will be more useful. Reported designs in [14], [31], and [32] has advantage of achieving independent pattern and polarization reconfiguration. However, in [14] the overall impedance and ARBW for each state is less than < 4%. Also, this antenna needs 48 PIN diodes which increases power consumption, loss, and complicates the DC biasing network.

It is observed that the reconfigurable antenna designs achieving beam steering with LP reconfiguration presented in [42], [72], [190], [191], and [192] achieves discrete beam switching. In [42] the radiated beam is switched only in H-plane with limited steering capability. The antenna design presented in [191] suffer from drawbacks such as the structure is non-planar, since the parasitic element is placed in the vertical plane and radiating patch in the horizontal plane. Furthermore, the antenna design does not allow for beam steering towards the broadside direction and exhibits a significantly narrow impedance bandwidth. The challenges associated with this category of antennas include realizing complete azimuthal coverage, enhanced beam steering capability, and a wide impedance bandwidth. In addition, it is noted that the pattern and polarization reconfigurable antenna designs achieving beam steering with CP reconfiguration realize pattern reconfigurability over a limited impedance and ARBW.

Table 8 provides an overview of the outcomes obtained from antenna designs that accomplish both beam steering along with the LP and CP reconfiguration. It is observed that the antenna design presented in [208] achieves a narrow impedance bandwidth of ∼1%. Three prototypes corresponding to LP configuration are fabricated. Also, this antenna needs large number of switches. The antenna design reported in [13] has large size and 60 PIN diodes are needed, which complicates DC biasing network. This antenna realizes discrete beam switching and complete 360° azimuth coverage is not obtained. Large gain variation is observed in [33], as main beam of the antenna is steered away from the

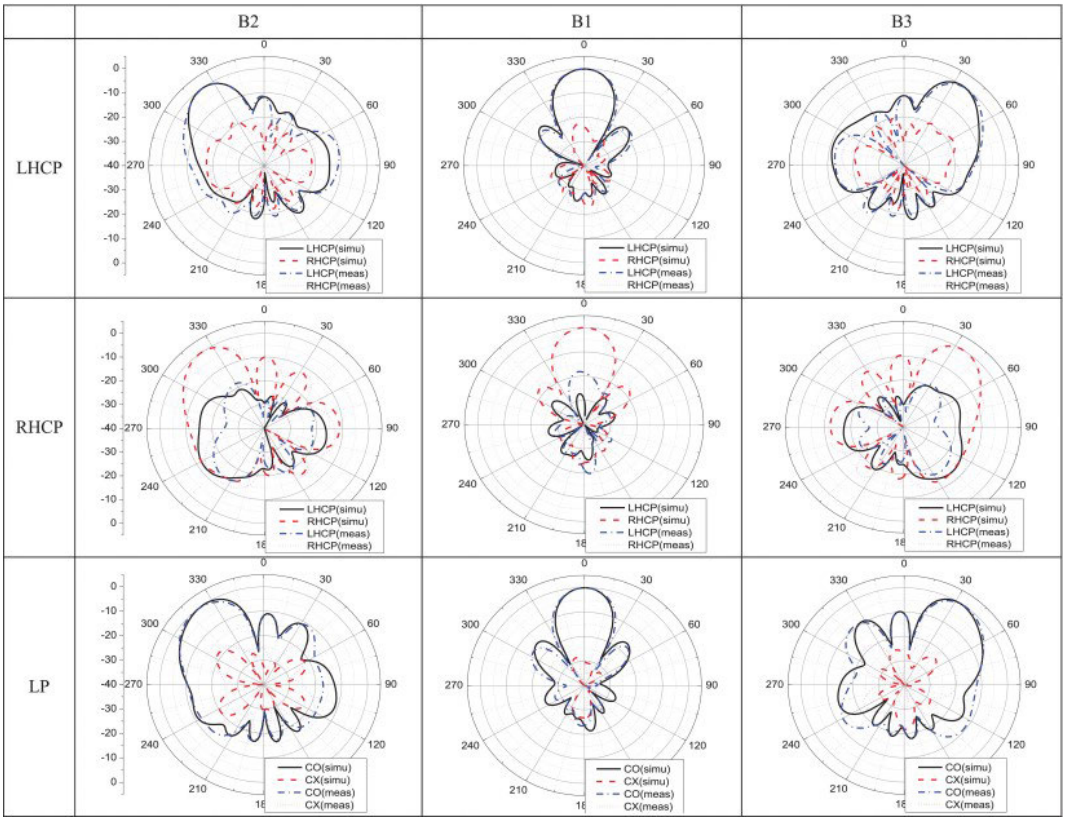

FIGURE 42. Normalized simulated and measured radiation pattern of the antenna array in the *xz*-plane at an operating frequency of 2.25 GHz [37].

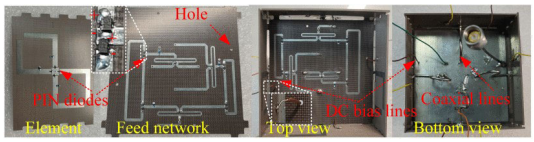

FIGURE 43. Fabricated 3-D pattern reconfigurable antenna array [212].

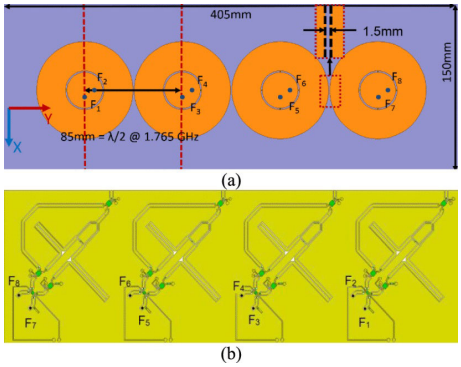

FIGURE 44. Geometry of the frequency agile 1 × 4 linear array antenna with its polarization feed network (PFN) (a) antenna array and (b) PFN exciting the radiating elements [38].

broadside direction. In [35] and [36] pattern and polarization of the antenna cannot be independently reconfigured. Also, in [35] broadside radiation is not obtained. Reconfigurable antenna design presented in [211] has certain limitations such as discrete beam switching, limited beam switching of ±20°, complete 360° azimuth coverage is not realized, and beam switching is not obtained with CP. The phased array developed in [38] is associated with complicated feeding network and beam steering is achieved only in the H-plane.

VIII. FUTURE RESEARCH DIRECTIONS

In future, there is potential for exploring the utilization of programmable metasurfaces and polarization conversion metasurfaces to achieve independent pattern and polarization reconfiguration. Pattern and polarization reconfigurable antennas need to possess the ability to achieve independent reconfiguration, wide impedance bandwidth, wide ARBW, enhanced beam steering, increased gain, and minimal variation in gain across different operating states. The challenge is also to design reconfigurable antenna with a low profile, low complexity, low cost, and easy integration with the feed networks. The pattern and polarization reconfigurable antennas should also be able to achieve 360° coverage with LP as well as CP reconfiguration over a wide operating bandwidth. Reconfigurable antennas can be effectively used in biomedical systems to give enhanced performance. These antennas can adjust the operating parameters based on requirements of various medical scenarios. However, there are certain challenges in terms of integration of antenna

TABLE 8. Performance comparison of pattern and polarization reconfigurable antenna designs achieving beam steering with LP and CP.

Ref.	Antenna type	Operating frequency (GHz)	360° azimuth coverage	Main beam elevation plane (degree)	Polarization	−10 dB BW (%)	3-dB AR BW (%)	Peak gain	Size (λ_0^3) (mm^3)	Switches (number)
[207]	Tunable parasitic	10.3	no	broadside, 4, ±19, ±10	LP LHCP	6.3	- 2.57	NA	NA	copper strips (8)
[208]	Parasitic pixel layer	5.25	no	−30, 0, 30	LP, CP	≈1	NA	8	1.05×1.05×0.036	copper strips (40)
[209]	Crossed-Yagi	4.02	yes	≈35	LVP, LHP LHCP, RHCP	5.96 5.91	- NA	8.68	1.88×1.88×0.02	copper strips (12)
[13]	Parasitic pixel layer	2.7	no	±30	LVP, LHP LHCP, RHCP	2.8	NA	4 (avg.)	2.16×1.08×0.068	PIN (60)
[33]	Tunable parasitic	2.45	yes	11 (xz-plane) 40 (yz-plane) 30	LVP, LHP LHCP, RHCP	1.6	1.6	2.24	1.14×1.14×0.026	varactor (16)
[210]	Metasurface	5	yes	±40 ±20 ±25	HP VP CP	16 18 27	NA	3.58 4.29 3.05	0.65×0.65×0.067	PIN (16)
[34]	Planar monopole	1.57	no	±15 ±25 L 30, R −30	LP LP LHCP, RHCP	4.4 1.9 3.5	- - 3.32	4.2	0.173×0.157×0.0084	PIN (4)
[35]	Rhombic patch	5.2 5.8	no	±30	±45 LP, LHCP, RHCP	3.59 3.5	- 3.5	3	1.04×2.6×0.028	PIN (6)
[36]	Patch-slot array	3.6 5.8	no	omni broadside broadside, ±30 broadside	Linear LHCP Linear RHCP	6.4 5.2	13.13 3.1	8.9	1.92×1.92×0.0192	PIN (10)
[211]	Patch with metal wall	3.3	no	±20 broadside	LP LHCP, RHCP	10.7	9.3	NA	0.47×0.47×0.152	PIN (12)
[37]	1×4 ME dipole array	2.25	no	±40	LP LHCP RHCP	18.2	10.9 11.55 11.2	8	0.48×0.60×0.263	varactor (2)

NA : Not available

with other subsystems, need of compact reconfigurable antennas, safety, energy efficient design, minimized electromagnetic interference (EMI), lower cost, low complexity, and sufficient communication range. The integration of reconfigurable antennas with other communication systems such as mm-wave and terahertz technologies possesses significant challenges. Moreover, incorporation of machine learning and artificial intelligence algorithms can make reconfigurable antennas more intelligent and adaptive to the environment. This approach can help to optimize the antenna parameters in real time and enhance the overall performance of wireless communication systems.

IX. CONCLUSION

A comprehensive review of multifunctional pattern and polarization reconfigurable antennas is presented. These multifunctional antennas are able to realize independent pattern and polarization reconfiguration in a single antenna structure. Furthermore, an extensive performance comparison of all the reported multifunctional pattern and polarization reconfigurable antennas is presented. Techniques used to achieve reconfiguration in antennas are reviewed in detail, along with the challenges faced at mm-wave frequencies. More research is needed regarding implementation of reconfigurable antenna using smart materials, liquid crystal based material for more efficient and flexible reconfiguration of antenna properties. Conventionally, phased arrays have been employed to enhance beam scanning capabilities, exhibiting excellent characteristics such as high gain, low side lobe level, low scan loss, and improved beam steering. However, utilization of phased arrays needs sophisticated feeding network design, precise engineering, and integration of complex elements. These arrays are linked to higher power requirements, increased costs, and larger physical dimensions. From the present review it can be concluded that very few reported antenna designs have addressed the challenge that is to achieve independent pattern and polarization reconfiguration in a compact antenna structure.

Once the antenna design is optimized for one polarization in one direction, scanning the main beam while keeping the sense of polarization remains a challenge.

REFERENCES

[1] D. Schaubert, F. Farrar, A. Sindoris, and S. Hayes, "Microstrip antennas with frequency agility and polarization diversity," *IEEE Trans. Antennas Propag.*, vol. AP-29, no. 1, pp. 118–123, Jan. 1981.

[2] N. Haider, D. Caratelli, and A. Yarovoy, "Recent developments in reconfigurable and multiband antenna technology," *Int. J. Antennas Propag.*, vol. 2013, no. 1, 2013, Art. no. 869170.

[3] A. C. K. Mak, C. R. Rowell, R. D. Murch, and C.-L. Mak, "Reconfigurable multiband antenna designs for wireless communication devices," *IEEE Trans. Antennas Propag.*, vol. 55, no. 7, pp. 1919–1928, Jul. 2007.

[4] S. Zhang, G. H. Huff, J. Feng, and J. T. Bernhard, "A pattern reconfigurable microstrip parasitic array," *IEEE Trans. Antennas Propag.*, vol. 52, no. 10, pp. 2773–2776, Oct. 2004.

[5] B. Kim, B. Pan, S. Nikolaou, Y.-S. Kim, J. Papapolymerou, and M. M. Tentzeris, "A novel single-feed circular microstrip antenna with reconfigurable polarization capability," *IEEE Trans. Antennas Propag.*, vol. 56, no. 3, pp. 630–638, Mar. 2008.

[6] G. H. Huff, J. Feng, S. Zhang, and J. T. Bernhard, "A novel radiation pattern and frequency reconfigurable single turn square spiral microstrip antenna," *IEEE Microw. Wireless Compon. Lett.*, vol. 13, no. 2, pp. 57–59, Feb. 2003.

[7] C. J. Panagamuwa, A. Chauraya, and J. C. Vardaxoglou, "Frequency and beam reconfigurable antenna using photoconducting switches," *IEEE Trans. Antennas Propag.*, vol. 54, no. 2, pp. 449–454, Feb. 2006.

[8] S. Nikolaou, R. Bairavasubramanian, C. Lugo, I. Carrasquillo, D. C. Thompson, G. E. Ponchak, J. Papapolymerou, and M. M. Tentzeris, "Pattern and frequency reconfigurable annular slot antenna using PIN diodes," *IEEE Trans. Antennas Propag.*, vol. 54, no. 2, pp. 439–448, Feb. 2006.

[9] T. Guo, W. Leng, A. Wang, J. Li, and Q. Zhang, "A novel planar parasitic array antenna with frequency- and pattern-reconfigurable characteristics," *IEEE Antennas Wireless Propag. Lett.*, vol. 13, pp. 1569–1572, 2014.

[10] P.-Y. Qin, Y. J. Guo, Y. Cai, E. Dutkiewicz, and C.-H. Liang, "A reconfigurable antenna with frequency and polarization agility," *IEEE Antennas Wireless Propag. Lett.*, vol. 10, pp. 1373–1376, 2011.

[11] N. Jin, F. Yang, and Y. Rahmat-Samii, "A novel patch antenna with switchable slot (PASS): Dual-frequency operation with reversed circular polarizations," *IEEE Trans. Antennas Propag.*, vol. 54, no. 3, pp. 1031–1034, Mar. 2006.

[12] W. L. Liu, T. R. Chen, S. H. Chen, and J. S. Row, "Reconfigurable microstrip antenna with pattern and polarisation diversities," *Electron. Lett.*, vol. 43, no. 2, pp. 77–78, Jan. 2007.

[13] D. Rodrigo, B. A. Cetiner, and L. Jofre, "Frequency, radiation pattern and polarization reconfigurable antenna using a parasitic pixel layer," *IEEE Trans. Antennas Propag.*, vol. 62, no. 6, pp. 3422–3427, Jun. 2014.

[14] L. Ge, Y. Li, J. Wang, and C.-Y.-D. Sim, "A low-profile reconfigurable cavity-backed slot antenna with frequency, polarization, and radiation pattern agility," *IEEE Trans. Antennas Propag.*, vol. 65, no. 5, pp. 2182–2189, May 2017.

[15] B. Dwivedy, S. K. Behera, and V. K. Singh, "A versatile triangular patch array for wideband frequency alteration with concurrent circular polarization and pattern reconfigurability," *IEEE Trans. Antennas Propag.*, vol. 67, no. 3, pp. 1640–1649, Mar. 2019.

[16] S. K. Sharma and J.-C. S. Chieh, *Multifunctional Antennas and Arrays for Wireless Communication Systems*. Hoboken, NJ, USA: Wiley, 2021.

[17] A. Khidre, F. Yang, and A. Z. Elsherbeni, "A patch antenna with a varactor-loaded slot for reconfigurable dual-band operation," *IEEE Trans. Antennas Propag.*, vol. 63, no. 2, pp. 755–760, Feb. 2015.

[18] A. Mansoul, F. Ghanem, M. R. Hamid, and M. Trabelsi, "A selective frequency-reconfigurable antenna for cognitive radio applications," *IEEE Antennas Wireless Propag. Lett.*, vol. 13, pp. 515–518, 2014.

[19] J. T. Bernhard, *Reconfigurable Antennas*. San Rafael, CA, USA: Morgan & Claypool, 2007.

[20] J. Hu, X. Yang, L. Ge, Z. Guo, Z.-C. Hao, and H. Wong, "A reconfigurable 1×4 circularly polarized patch array antenna with frequency, radiation pattern, and polarization agility," *IEEE Trans. Antennas Propag.*, vol. 69, no. 8, pp. 5124–5129, Jan. 2021.

[21] D. Piazza, P. Mookiah, M. D'Amico, and K. R. Dandekar, "Experimental analysis of pattern and polarization reconfigurable circular patch antennas for MIMO systems," *IEEE Trans. Veh. Technol.*, vol. 59, no. 5, pp. 2352–2362, Jun. 2010.

[22] W. Hong, K. Baek, and Y. Lee, "Quantitative analysis of the effects of polarization and pattern reconfiguration for mmWave 5G mobile antenna prototypes," in *Proc. IEEE Radio Wireless Symp. (RWS)*, Jan. 2017, pp. 68–71.

[23] W. Hong, "Solving the 5G mobile antenna puzzle: Assessing future directions for the 5G mobile antenna paradigm shift," *IEEE Microw. Mag.*, vol. 18, no. 7, pp. 86–102, Nov. 2017.

[24] Z. Jiajie, W. Anguo, and W. Peng, "A survey on reconfigurable antennas," in *Proc. Int. Conf. Microw. Millim. Wave Technol.*, vol. 3, Apr. 2008, pp. 1156–1159.

[25] J. Dong, Y. Li, and B. Zhang, "A survey on radiation pattern reconfigurable antennas," in *Proc. 7th Int. Conf. Wireless Commun., Netw. Mobile Comput.*, Sep. 2011, pp. 1–4.

[26] A. Chen, W. Jiang, Z. Chen, and J. Wang, "Overview on multipattern and multipolarization antennas for aerospace and terrestrial applications," *Int. J. Antennas Propag.*, vol. 2013, no. 1, 2013, Art. no. 102925.

[27] Y. J. Guo, P.-Y. Qin, S.-L. Chen, W. Lin, and R. W. Ziolkowski, "Advances in reconfigurable antenna systems facilitated by innovative technologies," *IEEE Access*, vol. 6, pp. 5780–5794, 2018.

[28] N. Ojaroudi Parchin, H. Jahanbakhsh Basherlou, Y. I. A. Al-Yasir, R. A. Abd-Alhameed, A. M. Abdulkhaleq, and J. M. Noras, "Recent developments of reconfigurable antennas for current and future wireless communication systems," *Electronics*, vol. 8, no. 2, p. 128, Jan. 2019.

[29] B. Cetiner, H. Jafarkhani, J.-Y. Qian, H. J. Yoo, A. Grau, and F. De Flaviis, "Multifunctional reconfigurable MEMS integrated antennas for adaptive MIMO systems," *IEEE Commun. Mag.*, vol. 42, no. 12, pp. 62–70, Dec. 2004.

[30] X. Liu, K. W. Leung, T. Zhang, N. Yang, P. Gu, and R. Chen, "An electrically controlled pattern- and polarization-reconfigurable cylindrical dielectric resonator antenna," *IEEE Antennas Wireless Propag. Lett.*, vol. 20, pp. 2309–2313, 2021.

[31] X. Yi, L. Huitema, and H. Wong, "Polarization and pattern reconfigurable cuboid quadrifilar helical antenna," *IEEE Trans. Antennas Propag.*, vol. 66, no. 6, pp. 2707–2715, Jun. 2018.

[32] P. Vasina, T. Mikulasek, J. Lacik, and H. Arthaber, "Beam- and polarisation-reconfigurable SIW ring-slot antenna array," *IET Microw., Antennas Propag.*, vol. 12, no. 15, pp. 2313–2319, 2018.

[33] V. V. Khairnar, C. Ramesha, and L. J. Gudino, "A parasitic antenna with independent pattern, beamwidth and polarization reconfigurability," *Wireless Pers. Commun.*, vol. 117, no. 3, pp. 2041–2059, 2021.

[34] M. M. Fakharian, P. Rezaei, and A. A. Orouji, "Polarization and radiation pattern reconfigurability of a planar monopole-fed loop antenna for GPS application," *Radioengineering*, vol. 25, no. 4, pp. 680–686, Dec. 2016.

[35] Y. P. Selvam, L. Elumalai, M. G. N. Alsath, M. Kanagasabai, S. Subbaraj, and S. Kingsly, "Novel frequency- and pattern-reconfigurable rhombic patch antenna with switchable polarization," *IEEE Antennas Wireless Propag. Lett.*, vol. 16, pp. 1639–1642, 2017.

[36] Y. Panneer Selvam, M. G. N. Alsath, M. Kanagasabai, L. Elumalai, S. K. Palaniswamy, S. Subbaraj, S. Kingsly, G. Konganathan, and I. Kulandhaisamy, "A patch-slot antenna array with compound reconfiguration," *IEEE Antennas Wireless Propag. Lett.*, vol. 17, pp. 525–528, 2018.

[37] J. Hu, X. Yang, L. Ge, and H. Wong, "A polarization and beam steering reconfigurable cavity-backed magneto-electric dipole antenna array using reflection-type phase shifter," *IEEE Trans. Antennas Propag.*, vol. 70, no. 1, pp. 296–306, Jan. 2022.

[38] B. Babakhani, S. K. Sharma, and N. R. Labadie, "A frequency agile microstrip patch phased array antenna with polarization reconfiguration," *IEEE Trans. Antennas Propag.*, vol. 64, no. 10, pp. 4316–4327, Oct. 2016.

[39] J. Hu and Z.-C. Hao, "A compact polarization-reconfigurable and 2-D beam-switchable antenna using the spatial phase shift technique," *IEEE Trans. Antennas Propag.*, vol. 66, no. 10, pp. 4986–4995, Oct. 2018.

[40] A. Bhattacharjee and S. Dwari, "A monopole antenna with reconfigurable circular polarization and pattern tilting ability in two switchable wide frequency bands," *IEEE Antennas Wireless Propag. Lett.*, vol. 20, no. 9, pp. 1661–1665, Sep. 2021.

[41] L. Kang, H. Li, X. Wang, J. Zhou, and J. Huang, "Circular polarization-agile and continuous beam-steerable array antenna using a hybrid design approach," *IEEE Trans. Antennas Propag.*, vol. 70, no. 2, pp. 1541–1546, Feb. 2022.

[42] S.-L. Chen, P.-Y. Qin, C. Ding, and Y. J. Guo, "Cavity-backed proximity-coupled reconfigurable microstrip antenna with agile polarizations and steerable beams," *IEEE Trans. Antennas Propag.*, vol. 65, no. 10, pp. 5553–5558, Oct. 2017.

[43] C. G. Christodoulou, Y. Tawk, S. A. Lane, and S. R. Erwin, "Reconfigurable antennas for wireless and space applications," *Proc. IEEE*, vol. 100, no. 7, pp. 2250–2261, Jul. 2012.

[44] S. Tang, Y. Zhang, Z. Han, C.-Y. Chiu, and R. Murch, "A pattern-reconfigurable antenna for single-RF 5G millimeter-wave communications," *IEEE Antennas Wireless Propag. Lett.*, vol. 20, no. 12, pp. 2344–2348, Sep. 2021.

[45] M. Patriotis, F. N. Ayoub, Y. Tawk, J. Costantine, and C. G. Christodoulou, "A four-element antenna array system with 15 reconfigurable radiation patterns," *IEEE Access*, vol. 9, pp. 108579–108585, 2021.

[46] L. Santamaria, F. Ferrero, R. Staraj, and L. Lizzi, "Slot-based pattern reconfigurable ESPAR antenna for IoT applications," *IEEE Trans. Antennas Propag.*, vol. 69, no. 7, pp. 3635–3644, Jul. 2021.

[47] X. Pan, F. Yang, S. Xu, and M. Li, "A 10 240-element reconfigurable reflectarray with fast steerable monopulse patterns," *IEEE Trans. Antennas Propag.*, vol. 69, no. 1, pp. 173–181, Jan. 2021.

[48] F. Meng, S. K. Sharma, and B. Babakhani, "A wideband frequency agile fork-shaped microstrip patch antenna with nearly invariant radiation patterns," *Int. J. RF Microw. Comput.-Aided Eng.*, vol. 26, no. 7, pp. 623–632, Sep. 2016.

[49] A. R. Vilenskiy, M. N. Makurin, C. Lee, and M. V. Ivashina, "Reconfigurable transmitarray with near-field coupling to gap waveguide array antenna for efficient 2-D beam steering," *IEEE Trans. Antennas Propag.*, vol. 68, no. 12, pp. 7854–7865, Dec. 2020.

[50] P. Bajaj, D. Kundu, and D. Singh, "SPICE-based modeling of a polarization-independent active frequency selective surface based tunable absorber with high angular stability," *Microw. Opt. Technol. Lett.*, vol. 66, no. 4, 2024, Art. no. e34140.

[51] T. S. Rappaport, S. Sun, R. Mayzus, H. Zhao, Y. Azar, K. Wang, G. N. Wong, J. K. Schulz, M. Samimi, and F. Gutierrez, "Millimeter wave mobile communications for 5G cellular: It will work!" *IEEE Access*, vol. 1, pp. 335–349, 2013.

[52] H. Pablo Zapata Cano, Z. D. Zaharis, T. V. Yioultsis, N. V. Kantartzis, and P. I. Lazaridis, "Pattern reconfigurable antennas at millimeter-wave frequencies: A comprehensive survey," *IEEE Access*, vol. 10, pp. 83029–83042, 2022.

[53] G. M. Rebeiz, *RF MEMS: Theory, Design, and Technology*. Hoboken, NJ, USA: Wiley, 2004.

[54] G. F. Engen and C. A. Hoer, "Thru-reflect-line: An improved technique for calibrating the dual six-port automatic network analyzer," *IEEE Trans. Microw. Theory Techn.*, vol. MTT-27, no. 12, pp. 987–993, Dec. 1979.

[55] K. Trzebiatowski, M. Rzymowski, L. Kulas, and K. Nyka, "Simple 60 GHz switched beam antenna for 5G millimeter-wave applications," *IEEE Antennas Wireless Propag. Lett.*, vol. 20, no. 1, pp. 38–42, Nov. 2021.

[56] C. Fan, B. Wu, Y. Hu, Y. Zhao, and T. Su, "Millimeter-wave pattern reconfigurable Vivaldi antenna using tunable resistor based on graphene," *IEEE Trans. Antennas Propag.*, vol. 68, no. 6, pp. 4939–4943, Jun. 2020.

[57] Z. Wu, H. Liu, and L. Li, "Metasurface-inspired low profile polarization reconfigurable antenna with simple DC controlling circuit," *IEEE Access*, vol. 7, pp. 45073–45079, 2019.

[58] S. V. Hum and H. Y. Xiong, "Analysis and design of a differentially-fed frequency agile microstrip patch antenna," *IEEE Trans. Antennas Propag.*, vol. 58, no. 10, pp. 3122–3130, Oct. 2010.

[59] V. V. Khairnar, B. V. Kadam, C. K. Ramesha, and L. J. Gudino, "A reconfigurable parasitic antenna with continuous beam scanning capability in H-plane," *AEU-Int. J. Electron. Commun.*, vol. 88, pp. 78–86, May 2018.

[60] I. F. da Costa, A. Cerqueira S., D. H. Spadoti, L. G. da Silva, J. A. J. Ribeiro, and S. E. Barbin, "Optically controlled reconfigurable antenna array for mm-wave applications," *IEEE Antennas Wireless Propag. Lett.*, vol. 16, pp. 2142–2145, 2017.

[61] S. Pendharker, R. K. Shevgaonkar, and A. N. Chandorkar, "Optically controlled frequency-reconfigurable microstrip antenna with low photoconductivity," *IEEE Antennas Wireless Propag. Lett.*, vol. 13, pp. 99–102, 2014.

[62] V. Sathi, N. Ehteshami, and J. Nourinia, "Optically tuned frequency-reconfigurable microstrip antenna," *IEEE Antennas Wireless Propag. Lett.*, vol. 11, pp. 1018–1020, 2012.

[63] D. Patron, A. S. Daryoush, and K. R. Dandekar, "Optical control of reconfigurable antennas and application to a novel pattern-reconfigurable planar design," *J. Lightw. Technol.*, vol. 32, no. 20, pp. 3394–3402, Oct. 15, 2014.

[64] S. J. Mazlouman, M. Soleimani, A. Mahanfar, C. Menon, and R. G. Vaughan, "Pattern reconfigurable square ring patch antenna actuated by hemispherical dielectric elastomer," *Electron. Lett.*, vol. 47, no. 3, pp. 164–165, Feb. 2011.

[65] G. Washington, H.-S. Yoon, M. Angelino, and W. H. Theunissen, "Design, modeling, and optimization of mechanically reconfigurable aperture antennas," *IEEE Trans. Antennas Propag.*, vol. 50, no. 5, pp. 628–637, May 2002.

[66] I. T. McMichael, "A mechanically reconfigurable patch antenna with polarization diversity," *IEEE Antennas Wireless Propag. Lett.*, vol. 17, no. 7, pp. 1186–1189, May 2018.

[67] H. L. Zhu, S. W. Cheung, and T. I. Yuk, "Mechanically pattern reconfigurable antenna using metasurface," *IET Microw., Antennas Propag.*, vol. 9, no. 12, pp. 1331–1336, 2015.

[68] A. Jouade, M. Himdi, A. Chauloux, and F. Colombel, "Mechanically pattern-reconfigurable bended horn antenna for high-power applications," *IEEE Antennas Wireless Propag. Lett.*, vol. 16, pp. 457–460, 2017.

[69] W. Hu, M. Y. Ismail, R. Cahill, J. A. Encinar, V. F. Fusco, H. S. Gamble, D. Linton, R. Dickie, N. Grant, and S. P. Rea, "Liquid-crystal-based reflectarray antenna with electronically switchable monopulse patterns," *Electron. Lett.*, vol. 43, no. 14, p. 744, 2007.

[70] D. M. Pozar and V. Sanchez, "Magnetic tuning of a microstrip antenna on a ferrite substrate," *Electron. Lett.*, vol. 24, no. 12, pp. 729–731, Jun. 1988.

[71] T. Zhang, Y. Chen, and S. Yang, "A wideband frequency- and polarization-reconfigurable liquid metal-based spiral antenna," *IEEE Antennas Wireless Propag. Lett.*, vol. 21, no. 7, pp. 1477–1481, May 2022.

[72] G. B. Zhang, R. C. Gough, M. R. Moorefield, K. J. Cho, A. T. Ohta, and W. A. Shiroma, "A liquid-metal polarization-pattern-reconfigurable dipole antenna," *IEEE Antennas Wireless Propag. Lett.*, vol. 17, pp. 50–53, 2018.

[73] A. Arbelaez, I. Goode, J. Gomez-Cruz, C. Escobedo, and C. E. Saavedra, "Liquid metal reconfigurable patch antenna for linear, RH, and LH circular polarization with frequency tuning," *Can. J. Electr. Comput. Eng.*, vol. 43, no. 4, pp. 218–223, Fall. 2020.

[74] X. Yang, Y. Liu, H. Lei, Y. Jia, P. Zhu, and Z. Zhou, "A radiation pattern reconfigurable Fabry–Pérot antenna based on liquid metal," *IEEE Trans. Antennas Propag.*, vol. 68, no. 11, pp. 7658–7663, Nov. 2020.

[75] J. Hao, J. Ren, X. Du, J. H. Mikkelsen, M. Shen, and Y. Z. Yin, "Pattern-reconfigurable Yagi–Uda antenna based on liquid metal," *IEEE Antennas Wireless Propag. Lett.*, vol. 20, no. 4, pp. 587–591, Feb. 2021.

[76] Z. Qu, J. R. Kelly, Z. Wang, S. Alkaraki, and Y. Gao, "A reconfigurable microstrip patch antenna with switchable liquid-metal ground plane," *IEEE Antennas Wireless Propag. Lett.*, vol. 22, no. 5, pp. 1045–1049, Dec. 2023.

[77] X. H. Wang, H. W. Pan, L. Z. Wang, X. W. Shi, and Y. Xu, "A simple frequency- and polarization-reconfigurable bent monopole antenna based on liquid metal," *IEEE Antennas Wireless Propag. Lett.*, vol. 22, no. 5, pp. 950–954, May 2023.

[78] L. Li, X. Yan, H. C. Zhang, and Q. Wang, "Polarization- and frequency-reconfigurable patch antenna using gravity-controlled liquid metal," *IEEE Trans. Circuits Syst. II: Exp. Briefs*, vol. 69, no. 3, pp. 1029–1033, Mar. 2022.

[79] M. Wang, I. M. Kilgore, M. B. Steer, and J. J. Adams, "Characterization of intermodulation distortion in reconfigurable liquid metal antennas," *IEEE Antennas Wireless Propag. Lett.*, vol. 17, no. 2, pp. 279–282, Dec. 2018.

[80] Z. Li, E. Ahmed, A. M. Eltawil, and B. A. Cetiner, "A beam-steering reconfigurable antenna for WLAN applications," *IEEE Trans. Antennas Propag.*, vol. 63, no. 1, pp. 24–32, Jan. 2015.

[81] Md. A. Towfiq, I. Bahceci, S. Blanch, J. Romeu, L. Jofre, and B. A. Cetiner, "A reconfigurable antenna with beam steering and beamwidth variability for wireless communications," *IEEE Trans. Antennas Propag.*, vol. 66, no. 10, pp. 5052–5063, Oct. 2018.

[82] Y. You, K. L. Ford, J. M. Rigelsford, and T. O'Farrell, "Systems analysis of a pattern reconfigurable antenna for capacity improvement of cell edge users in cellular networks," *IEEE Trans. Veh. Technol.*, vol. 67, no. 12, pp. 11848–11857, Dec. 2018.

[83] H. Kunsei, K. S. Bialkowski, M. S. Alam, and A. M. Abbosh, "Improved communications in underground mines using reconfigurable antennas," *IEEE Trans. Antennas Propag.*, vol. 66, no. 12, pp. 7505–7510, Dec. 2018.

[84] S. Jeong and W. J. Chappell, "A city-wide smart wireless sewer sensor network using parasitic slot array antennas," *IEEE Antennas Wireless Propag. Lett.*, vol. 9, pp. 760–763, 2010.

[85] A. Darvazehban, S. Ahdi Rezaeieh, A. Zamani, and A. M. Abbosh, "Pattern reconfigurable metasurface antenna for electromagnetic torso imaging," *IEEE Trans. Antennas Propag.*, vol. 67, no. 8, pp. 5453–5462, Aug. 2019.

[86] S. Wolfe, S. Begashaw, Y. Liu, and K. R. Dandekar, "Adaptive link optimization for 802.11 UAV uplink using a reconfigurable antenna," in *Proc. IEEE Mil. Commun. Conf. (MILCOM)*, Oct. 2018, pp. 1–6.

[87] M. Burtowy, M. Rzymowski, and L. Kulas, "Low-profile ESPAR antenna for RSS-based DoA estimation in IoT applications," *IEEE Access*, vol. 7, pp. 17403–17411, 2019.

[88] A. Khidre, F. Yang, and A. Z. Elsherbeni, "Circularly polarized beam-scanning microstrip antenna using a reconfigurable parasitic patch of tunable electrical size," *IEEE Trans. Antennas Propag.*, vol. 63, no. 7, pp. 2858–2866, Jul. 2015.

[89] A. D. Johnson, V. Manohar, S. B. Venkatakrishnan, and J. L. Volakis, "Low-cost S-band reconfigurable monopole/patch antenna for CubeSats," *IEEE Open J. Antennas Propag.*, vol. 1, pp. 598–603, 2020.

[90] M. Ali, A. T. M. Sayem, and V. K. Kunda, "A reconfigurable stacked microstrip patch antenna for satellite and terrestrial links," *IEEE Trans. Veh. Technol.*, vol. 56, no. 2, pp. 426–435, Mar. 2007.

[91] V. V. Khairnar, B. V. Kadam, C. K. Ramesha, and L. J. Gudino, "A reconfigurable microstrip cross parasitic antenna with complete azimuthal beam scanning and tunable beamwidth," *Int. J. RF Microw. Comput.-Aided Eng.*, vol. 29, no. 1, Jan. 2019, Art. no. e21472.

[92] J. Li, Q. Zeng, R. Liu, and T. A. Denidni, "Beam-tilting antenna with negative refractive index metamaterial loading," *IEEE Antennas Wireless Propag. Lett.*, vol. 16, pp. 2030–2033, 2017.

[93] R. Guzman-Quiros, J. Luis Gomez-Tornero, A. R. Weily, and Y. Jay Guo, "Electronic full-space scanning with 1-D Fabry–Pérot LWA using electromagnetic band-gap," *IEEE Antennas Wireless Propag. Lett.*, vol. 11, pp. 1426–1429, 2012.

[94] S. S. I. Mitu and F. Sultan, "Beam scanning properties of a ferrite loaded microstrip patch antenna," *Int. J. Antennas Propag.*, vol. 2015, no. 1, 2015, Art. no. 697409.

[95] L.-Y. Ji, Y. J. Guo, P.-Y. Qin, S.-X. Gong, and R. Mittra, "A reconfigurable partially reflective surface (PRS) antenna for beam steering," *IEEE Trans. Antennas Propag.*, vol. 63, no. 6, pp. 2387–2395, Jun. 2015.

[96] Y. Yusuf and X. Gong, "A low-cost patch antenna phased array with analog beam steering using mutual coupling and reactive loading," *IEEE Antennas Wireless Propag. Lett.*, vol. 7, pp. 81–84, 2008.

[97] J. J. Luther, S. Ebadi, and X. Gong, "A microstrip patch electronically steerable parasitic array radiator (ESPAR) antenna with reactance-tuned coupling and maintained resonance," *IEEE Trans. Antennas Propag.*, vol. 60, no. 4, pp. 1803–1813, Apr. 2012.

[98] S. V. S. Nair and M. J. Ammann, "Reconfigurable antenna with elevation and azimuth beam switching," *IEEE Antennas Wireless Propag. Lett.*, vol. 9, pp. 367–370, 2010.

[99] C.-C. Hu, C. F. Jou, and J.-J. Wu, "A two-dimensional beam-scanning linear active leaky-wave antenna array," *IEEE Microw. Guided Wave Lett.*, vol. 9, no. 3, pp. 102–104, Mar. 1999.

[100] D. F. Sievenpiper, J. H. Schaffner, H. J. Song, R. Y. Loo, and G. Tangonan, "Two-dimensional beam steering using an electrically tunable impedance surface," *IEEE Trans. Antennas Propag.*, vol. 51, no. 10, pp. 2713–2722, Oct. 2003.

[101] M. Bouslama, M. Traii, T. A. Denidni, and A. Gharsallah, "Beam-switching antenna with a new reconfigurable frequency selective surface," *IEEE Antennas Wireless Propag. Lett.*, vol. 15, pp. 1159–1162, 2016.

[102] A. Khidre, F. Yang, and A. Z. Elsherbeni, "Reconfigurable microstrip antenna with two-dimensional scannable beam," in *Proc. IEEE Antennas Propag. Soc. Int. Symp. (APSURSI)*, Jul. 2013, pp. 196–197.

[103] B. Tsai and S.-Y. Chen, "Design of beam-steerable parasitic patch arrays using variable reactive loads," in *Proc. IEEE 4th Asia–Pacific Conf. Antennas Propag. (APCAP)*, Jun. 2015, pp. 423–424.

[104] W. Ouyang and X. Gong, "Cavity-backed slot ESPAR cross array with two-dimensional beam steering control," in *Proc. IEEE Int. Symp. Antennas Propag. USNC/URSI Nat. Radio Sci. Meeting*, Jul. 2017, pp. 307–308.

[105] R. Movahedinia, M. R. Chaharmir, A. R. Sebak, M. Ranjbar Nikkhah, and A. A. Kishk, "Realization of large dielectric resonator antenna ESPAR," *IEEE Trans. Antennas Propag.*, vol. 65, no. 7, pp. 3744–3749, Jul. 2017.

[106] S. Jeong, D. Ha, and W. J. Chappell, "A planar parasitic array antenna for tunable radiation pattern," in *Proc. IEEE Antennas Propag. Soc. Int. Symp.*, Jun. 2009, pp. 1–4.

[107] Y. Urata, M. Haneishi, and Y. Kimura, "Beam-adjustable planar arrays composed of microstrip antennas," *Electron. Commun. Jpn. (II, Electron.)*, vol. 87, no. 10, pp. 1–12, 2004.

[108] M. Jusoh, T. Sabapathy, M. F. Jamlos, and M. R. Kamarudin, "Reconfigurable four-parasitic-elements patch antenna for high-gain beam switching application," *IEEE Antennas Wireless Propag. Lett.*, vol. 13, pp. 79–82, 2014.

[109] M. Jusoh, T. Aboufoul, T. Sabapathy, A. Alomainy, and M. Ramlee Kamarudin, "Pattern-reconfigurable microstrip patch antenna with multidirectional beam for Wimax application," *IEEE Antennas Wireless Propag. Lett.*, vol. 13, pp. 860–863, 2014.

[110] Y. Yang and X. Zhu, "A wideband reconfigurable antenna with 360° beam steering for 802.11ac WLAN applications," *IEEE Trans. Antennas Propag.*, vol. 66, no. 2, pp. 600–608, Feb. 2018.

[111] M. S. Alam and A. M. Abbosh, "Beam-steerable planar antenna using circular disc and four PIN-controlled tapered stubs for Wimax and WLAN applications," *IEEE Antennas Wireless Propag. Lett.*, vol. 15, pp. 980–983, 2016.

[112] M. S. Alam and A. M. Abbosh, "Planar pattern reconfigurable antenna with eight switchable beams for WiMax and WLAN applications," *IET Microw., Antennas Propag.*, vol. 10, no. 10, pp. 1030–1035, 2016.

[113] M. S. Alam and A. M. Abbosh, "Wideband pattern-reconfigurable antenna using pair of radial radiators on truncated ground with switchable director and reflector," *IEEE Antennas Wireless Propag. Lett.*, vol. 16, pp. 24–28, 2017.

[114] P. Lotfi, S. Soltani, and R. D. Murch, "Broadside beam-steerable planar parasitic pixel patch antenna," *IEEE Trans. Antennas Propag.*, vol. 64, no. 10, pp. 4519–4524, Oct. 2016.

[115] M. S. Alam, Y. Wang, N. Nguyen-Trong, and A. Abbosh, "Compact circular reconfigurable antenna for high directivity and 360° beam scanning," *IEEE Antennas Wireless Propag. Lett.*, vol. 17, pp. 1492–1496, 2018.

[116] S.-L. Chen, P.-Y. Qin, W. Lin, and Y. J. Guo, "Pattern-reconfigurable antenna with five switchable beams in elevation plane," *IEEE Antennas Wireless Propag. Lett.*, vol. 17, no. 3, pp. 454–457, Mar. 2018.

[117] R. Guzmán-Quirós, A. R. Weily, J. L. Gómez-Tornero, and Y. J. Guo, "A Fabry–Pérot antenna with two-dimensional electronic beam scanning," *IEEE Trans. Antennas Propag.*, vol. 64, no. 4, pp. 1536–1541, Apr. 2016.

[118] A. Dadgarpour, B. Zarghooni, B. S. Virdee, and T. A. Denidni, "One- and two-dimensional beam-switching antenna for millimeter-wave MIMO applications," *IEEE Trans. Antennas Propag.*, vol. 64, no. 2, pp. 564–573, Feb. 2016.

[119] L. Ge, K. M. Luk, and S. Chen, "360° beam-steering reconfigurable wideband substrate integrated waveguide horn antenna," *IEEE Trans. Antennas Propag.*, vol. 64, no. 12, pp. 5005–5011, Dec. 2016.

[120] Z.-L. Lu, X.-X. Yang, and G.-N. Tan, "A multidirectional pattern-reconfigurable patch antenna with CSRR on the ground," *IEEE Antennas Wireless Propag. Lett.*, vol. 16, pp. 416–419, 2017.

[121] Y. Li and K.-M. Luk, "A linearly polarized magnetoelectric dipole with wide H-plane beamwidth," *IEEE Trans. Antennas Propag.*, vol. 62, no. 4, pp. 1830–1836, Apr. 2014.

[122] L. Ge and K. M. Luk, "A three-element linear magneto-electric dipole array with beamwidth reconfiguration," *IEEE Antennas Wireless Propag. Lett.*, vol. 14, pp. 28–31, 2015.

[123] L. Ge and K.-M. Luk, "Linearly polarized and dual-polarized magneto-electric dipole antennas with reconfigurable beamwidth in the H-plane," *IEEE Trans. Antennas Propag.*, vol. 64, no. 2, pp. 423–431, Feb. 2016.

[124] L. Ge and K. M. Luk, "Beamwidth reconfigurable magneto-electric dipole antenna based on tunable strip grating reflector," *IEEE Access*, vol. 4, pp. 7039–7045, 2016.

[125] B. Feng, Y. Tu, K. L. Chung, and Q. Zeng, "A beamwidth reconfigurable antenna array with triple dual-polarized magneto-electric dipole elements," *IEEE Access*, vol. 6, pp. 36083–36091, 2018.

[126] Y. Shi, Y. Cai, J. Yang, and L. Li, "A magnetoelectric dipole antenna with beamwidth reconfiguration," *IEEE Antennas Wireless Propag. Lett.*, vol. 18, no. 4, pp. 621–625, Apr. 2019.

[127] A. Edalati and T. A. Denidni, "Reconfigurable beamwidth antenna based on active partially reflective surfaces," *IEEE Antennas Wireless Propag. Lett.*, vol. 8, pp. 1087–1090, 2009.

[128] T. Debogovic, J. Perruisseau-Carrier, and J. Bartolic, "Partially reflective surface antenna with dynamic beamwidth control," *IEEE Antennas Wireless Propag. Lett.*, vol. 9, pp. 1157–1160, 2010.

[129] T. Debogovic, J. Bartolic, and J. Perruisseau-Carrier, "Dual-polarized partially reflective surface antenna with MEMS-based beamwidth reconfiguration," *IEEE Trans. Antennas Propag.*, vol. 62, no. 1, pp. 228–236, Jan. 2014.

[130] I. A. Korisch and B. Rulf, "Antenna beamwidth control using parasitic subarrays," in *Proc. IEEE-APS Conf. Antennas Propag. Wireless Commun.*, Nov. 2000, pp. 117–120.

[131] A. Khidre, F. Yang, and A. Z. Elsherbeni, "Reconfigurable microstrip antenna with tunable radiation beamwidth," in *Proc. IEEE Antennas Propag. Soc. Int. Symp. (APSURSI)*, Jul. 2013, pp. 1444–1445.

[132] M. Saitoh, N. Honma, and T. Murakami, "Impact of radiation pattern control of MIMO antenna on interfered multicell environment," *IEEE Antennas Wireless Propag. Lett.*, vol. 15, pp. 666–669, 2016.

[133] S.-N. Lee, J. Kim, J.-G. Yook, Y. Charlie Hu, and D. Peroulis, "A variable beamwidth antenna for wireless mesh networks," in *Proc. IEEE Antennas Propag. Soc. Int. Symp.*, Jun. 2007, pp. 493–496.

[134] H. N. Chu and T.-G. Ma, "Beamwidth switchable planar microstrip series-fed slot array using reconfigurable synthesized transmission lines," *IEEE Trans. Antennas Propag.*, vol. 65, no. 7, pp. 3766–3771, Jul. 2017.

[135] D.-W. Kim and S.-S. Oh, "Design of a coupler with three reconfigurable output ports and a beamwidth reconfigurable antenna," *Int. J. Antennas Propag.*, vol. 2017, no. 1, 2017, Art. no. 3490171.

[136] C.-W. Tsai and J.-S. Row, "Beamwidth reconfigurable slotted-patch antennas," in *Proc. IEEE 5th Asia–Pacific Conf. Antennas Propag. (APCAP)*, Jul. 2016, pp. 149–150.

[137] M. Wang, C. Huang, P. Chen, Y. Wang, Z. Zhao, and X. Luo, "Controlling beamwidth of antenna using frequency selective surface superstrate," *IEEE Antennas Wireless Propag. Lett.*, vol. 13, pp. 213–216, 2014.

[138] J. Zhang, S. Zhang, and G. F. Pedersen, "E-plane beam width reconfigurable dipole antenna with tunable parasitic strip," in *Proc. 12th Eur. Conf. Antennas Propag. (EuCAP)*, Apr. 2018, pp. 1–3.

[139] M. Shaw and Y. K. Choukiker, "Reconfigurable polarization and pattern microstrip antenna for IRNSS band applications," *AEU-Int. J. Electron. Commun.*, vol. 160, Feb. 2023, Art. no. 154501.

[140] T. Debogovic and J. Perruisseau-Carrier, "Array-fed partially reflective surface antenna with independent scanning and beamwidth dynamic control," *IEEE Trans. Antennas Propag.*, vol. 62, no. 1, pp. 446–449, Jan. 2014.

[141] G. Yang, J. Li, D. Wei, S. Zhou, and R. Xu, "Pattern reconfigurable microstrip antenna with multidirectional beam for wireless communication," *IEEE Trans. Antennas Propag.*, vol. 67, no. 3, pp. 1910–1915, Mar. 2019.

[142] J. Wang, J. Yin, H. Wang, C. Yu, and W. Hong, "Wideband U-slot patch antenna with reconfigurable radiation pattern," in *Proc. 11th Eur. Conf. Antennas Propag. (EUCAP)*, Mar. 2017, pp. 611–615.

[143] W.-Q. Deng, X.-S. Yang, C.-S. Shen, J. Zhao, and B.-Z. Wang, "A dual-polarized pattern reconfigurable Yagi patch antenna for microbase stations," *IEEE Trans. Antennas Propag.*, vol. 65, no. 10, pp. 5095–5102, Oct. 2017.

[144] S. Lim, C. Caloz, and T. Itoh, "Metamaterial-based electronically controlled transmission-line structure as a novel leaky-wave antenna with tunable radiation angle and beamwidth," *IEEE Trans. Microw. Theory Techn.*, vol. 53, no. 1, pp. 161–173, Jan. 2005.

[145] T. Liang, Z. Wang, and Y. Dong, "A beamwidth and steering reconfigurable active integrated metasurface antenna for dynamic radiation control," *IEEE Trans. Antennas Propag.*, vol. 70, no. 10, pp. 9006–9016, Oct. 2022.

[146] L. L. Sheng, W. P. Cao, L. R. Mei, and X. H. Yu, "A novel low-cost beam-controlling antenna based on digital coding metasurface," *Int. J. RF Microw. Comput.-Aided Eng.*, vol. 32, no. 6, 2022, Art. no. e23152.

[147] Z. Zhang, S. Cao, and J. Wang, "Azimuth-pattern reconfigurable planar antenna design using characteristic mode analysis," *IEEE Access*, vol. 9, pp. 60043–60051, 2021.

[148] Y. Dong and T. Itoh, "Metamaterial-based antennas," *Proc. IEEE*, vol. 100, no. 7, pp. 2271–2285, Jul. 2012.

[149] C. L. Holloway, E. F. Kuester, J. A. Gordon, J. O'Hara, J. Booth, and D. R. Smith, "An overview of the theory and applications of metasurfaces: The two-dimensional equivalents of metamaterials," *IEEE Antennas Propag. Mag.*, vol. 54, no. 2, pp. 10–35, Apr. 2012.

[150] R. W. Ziolkowski, "Design, fabrication, and testing of double negative metamaterials," *IEEE Trans. Antennas Propag.*, vol. 51, no. 7, pp. 1516–1529, Jul. 2003.

[151] N. Engheta, "An idea for thin subwavelength cavity resonators using metamaterials with negative permittivity and permeability," *IEEE Antennas Wireless Propag. Lett.*, vol. 1, pp. 10–13, 2002.

[152] R. W. Ziolkowski and A. Erentok, "Metamaterial-based efficient electrically small antennas," *IEEE Trans. Antennas Propag.*, vol. 54, no. 7, pp. 2113–2130, Jul. 2006.

[153] T. J. Cui, M. Q. Qi, X. Wan, J. Zhao, and Q. Cheng, "Coding metamaterials, digital metamaterials and programmable metamaterials," *Light: Sci. Appl.*, vol. 3, no. 10, p. e218, Oct. 2014.

[154] Y. F. Cao and X. Y. Zhang, "A wideband beam-steerable slot antenna using artificial magnetic conductors with simple structure," *IEEE Trans. Antennas Propag.*, vol. 66, no. 4, pp. 1685–1694, Apr. 2018.

[155] H. Wong, W. Lin, L. Huitema, and E. Arnaud, "Multi-polarization reconfigurable antenna for wireless biomedical system," *IEEE Trans. Biomed. Circuits Syst.*, vol. 11, no. 3, pp. 652–660, Jun. 2017.

[156] Q. Chen, J.-Y. Li, G. Yang, B. Cao, and Z. Zhang, "A polarization-reconfigurable high-gain microstrip antenna," *IEEE Trans. Antennas Propag.*, vol. 67, no. 5, pp. 3461–3466, May 2019.

[157] L. Kang, H. Li, J. Zhou, and S. Zheng, "An OAM-mode reconfigurable array antenna with polarization agility," *IEEE Access*, vol. 8, pp. 40445–40452, 2020.

[158] D. Chen, Y. Liu, S.-L. Chen, P.-Y. Qin, and Y. J. Guo, "A wideband high-gain multilinear polarization reconfigurable antenna," *IEEE Trans. Antennas Propag.*, vol. 69, no. 7, pp. 4136–4141, Jul. 2021.

[159] X. Liu, K. W. Leung, and N. Yang, "Wideband horizontally polarized omnidirectional cylindrical dielectric resonator antenna for polarization reconfigurable design," *IEEE Trans. Antennas Propag.*, vol. 69, no. 11, pp. 7333–7342, Nov. 2021.

[160] A. Khidre, K.-F. Lee, F. Yang, and A. Z. Elsherbeni, "Circular polarization reconfigurable wideband E-shaped patch antenna for wireless applications," *IEEE Trans. Antennas Propag.*, vol. 61, no. 2, pp. 960–964, Feb. 2013.

[161] W. Lin and H. Wong, "Wideband circular-polarization reconfigurable antenna with L-shaped feeding probes," *IEEE Antennas Wireless Propag. Lett.*, vol. 16, pp. 2114–2117, 2017.

[162] B. Li and Q. Xue, "Polarization-reconfigurable omnidirectional antenna combining dipole and loop radiators," *IEEE Antennas Wireless Propag. Lett.*, vol. 12, pp. 1102–1105, 2013.

[163] P. Kumar, S. Dwari, R. K. Saini, and M. K. Mandal, "Dual-band dual-sense polarization reconfigurable circularly polarized antenna," *IEEE Antennas Wireless Propag. Lett.*, vol. 18, no. 1, pp. 64–68, Jan. 2019.

[164] W. Li, S. Gao, Y. Cai, Q. Luo, M. Sobhy, G. Wei, J. Xu, J. Li, C. Wu, and Z. Cheng, "Polarization-reconfigurable circularly polarized planar antenna using switchable polarizer," *IEEE Trans. Antennas Propag.*, vol. 65, no. 9, pp. 4470–4477, Sep. 2017.

[165] Z. Chen, H.-Z. Li, H. Wong, X. Zhang, and T. Yuan, "A circularly-polarized-reconfigurable patch antenna with liquid dielectric," *IEEE Open J. Antennas Propag.*, vol. 2, pp. 396–401, 2021.

[166] H. H. Tran, C. D. Bui, N. Nguyen-Trong, and T. K. Nguyen, "A wideband non-uniform metasurface-based circularly polarized reconfigurable antenna," *IEEE Access*, vol. 9, pp. 42325–42332, 2021.

[167] P.-Y. Qin, A. R. Weily, Y. J. Guo, and C.-H. Liang, "Polarization reconfigurable U-slot patch antenna," *IEEE Trans. Antennas Propag.*, vol. 58, no. 10, pp. 3383–3388, Oct. 2010.

[168] M. S. Nishamol, V. P. Sarin, D. Tony, C. K. Aanandan, P. Mohanan, and K. Vasudevan, "An electronically reconfigurable microstrip antenna with switchable slots for polarization diversity," *IEEE Trans. Antennas Propag.*, vol. 59, no. 9, pp. 3424–3427, Sep. 2011.

[169] Z.-X. Yang, H.-C. Yang, J.-S. Hong, and Y. Li, "Bandwidth enhancement of a polarization-reconfigurable patch antenna with stair-slots on the ground," *IEEE Antennas Wireless Propag. Lett.*, vol. 13, pp. 579–582, 2014.

[170] A. Bhattacharjee, S. Dwari, and M. K. Mandal, "Polarization-reconfigurable compact monopole antenna with wide effective bandwidth," *IEEE Antennas Wireless Propag. Lett.*, vol. 18, no. 5, pp. 1041–1045, May 2019.

[171] L. Kang, H. Li, B. Tang, X. Wang, and J. Zhou, "Quad-polarization-reconfigurable antenna with a compact and switchable feed," *IEEE Antennas Wireless Propag. Lett.*, vol. 20, no. 4, pp. 548–552, Apr. 2021.

[172] J. Hu, G. Q. Luo, and Z.-C. Hao, "A wideband quad-polarization reconfigurable metasurface antenna," *IEEE Access*, vol. 6, pp. 6130–6137, 2018.

[173] P. Liu, W. Jiang, S. Sun, Y. Xi, and S. Gong, "Broadband and low-profile penta-polarization reconfigurable metamaterial antenna," *IEEE Access*, vol. 8, pp. 21823–21831, 2020.

[174] M. Li, Z. Zhang, M.-C. Tang, L. Zhu, and N.-W. Liu, "Bandwidth enhancement and size reduction of a low-profile polarization-reconfigurable antenna by utilizing multiple resonances," *IEEE Trans. Antennas Propag.*, vol. 70, no. 2, pp. 1517–1522, Feb. 2022.

[175] M. Li, Z. Zhang, and M.-C. Tang, "A compact, low-profile, wideband, electrically controlled, tri-polarization-reconfigurable antenna with quadruple gap-coupled patches," *IEEE Trans. Antennas Propag.*, vol. 68, no. 8, pp. 6395–6400, Aug. 2020.

[176] J. L. Valdes, L. Huitema, E. Arnaud, D. Passerieux, and A. Crunteanu, "A polarization reconfigurable patch antenna in the millimeter-waves domain using optical control of phase change materials," *IEEE Open J. Antennas Propag.*, vol. 1, pp. 224–232, 2020.

[177] W. Cao, B. Zhang, A. Liu, T. Yu, D. Guo, and K. Pan, "A reconfigurable microstrip antenna with radiation pattern selectivity and polarization diversity," *IEEE Antennas Wireless Propag. Lett.*, vol. 11, pp. 453–456, 2012.

[178] F. Sun, F. Zhang, and C. Feng, "A microstrip antenna for polarized diversity and pattern selectivity application," in *Proc. Int. Conf. Microw. Millim. Wave Technol. (ICMMT)*, May 2018, pp. 1–4.

[179] Y. Yang, R. B. V. B. Simorangkir, X. Zhu, K. Esselle, and Q. Xue, "A novel boresight and conical pattern reconfigurable antenna with the diversity of 360° polarization scanning," *IEEE Trans. Antennas Propag.*, vol. 65, no. 11, pp. 5747–5756, Nov. 2017.

[180] J.-S. Row and Y.-J. Huang, "Reconfigurable antenna with switchable broadside and conical beams and switchable linear polarized patterns," *IEEE Trans. Antennas Propag.*, vol. 66, no. 7, pp. 3752–3756, Jul. 2018.

[181] N. Nguyen-Trong, A. T. Mobashsher, and A. M. Abbosh, "Reconfigurable shorted patch antenna with polarization and pattern diversity," in *Proc. Austral. Microw. Symp. (AMS)*, Feb. 2018, pp. 27–28.

[182] M. Hwang, G. Kim, S. Kim, and N. S. Jeong, "Origami-inspired radiation pattern and shape reconfigurable dipole array antenna at C-band for CubeSat applications," *IEEE Trans. Antennas Propag.*, vol. 69, no. 5, pp. 2697–2705, May 2021.

[183] J. Ren, Z. Zhou, Z. H. Wei, H. M. Ren, Z. Chen, Y. Liu, and Y. Z. Yin, "Radiation pattern and polarization reconfigurable antenna using dielectric liquid," *IEEE Trans. Antennas Propag.*, vol. 68, no. 12, pp. 8174–8179, Dec. 2020.

[184] S. Raman, P. Mohanan, N. Timmons, and J. Morrison, "Microstrip-fed pattern- and polarization- reconfigurable compact truncated monopole antenna," *IEEE Antennas Wireless Propag. Lett.*, vol. 12, pp. 710–713, 2013.

[185] C. Sulakshana and L. Anjaneyulu, "A compact reconfigurable antenna with frequency, polarization and pattern diversity," *J. Electromagn. Waves Appl.*, vol. 29, no. 15, pp. 1953–1964, Oct. 2015.

[186] K. Yang, A. Loutridis, X. Bao, G. Ruvio, and M. J. Ammann, "Printed inverted-F antenna with reconfigurable pattern and polarization," in *Proc. 10th Eur. Conf. Antennas Propag. (EuCAP)*, Apr. 2016, pp. 1–5.

[187] A. Narbudowicz, X. Bao, and M. J. Ammann, "Omnidirectional microstrip patch antenna with reconfigurable pattern and polarisation," *IET Microw., Antennas Propag.*, vol. 8, no. 11, pp. 872–877, 2014.

[188] W. Chen, J. Sun, and Z. Feng, "A novel compact reconfigurable polarization and pattern antenna," *Microw. Opt. Technol. Lett.*, vol. 49, no. 11, pp. 2802–2805, Nov. 2007.

[189] C. Hua, S. Wang, Z. Hu, Z. Zhu, Z. Ren, W. Wu, and Z. Shen, "Reconfigurable antennas based on pure water," *IEEE Open J. Antennas Propag.*, vol. 2, pp. 623–633, 2021.

[190] A. N'gom, A. Diallo, K. Talla, A. Chaibo, I. Dioum, J. M. Ribero, and A. C. Beye, "A reconfigurable beam dual polarized microstrip cross patch antenna," in *Proc. 11th Eur. Conf. Antennas Propag. (EUCAP)*, Mar. 2017, pp. 3135–3139.

[191] C. Gu, S. Gao, H. Liu, Q. Luo, T.-H. Loh, M. Sobhy, J. Li, G. Wei, J. Xu, F. Qin, B. Sanz-Izquierdo, and R. A. Abd-Alhameed, "Compact smart antenna with electronic beam-switching and reconfigurable polarizations," *IEEE Trans. Antennas Propag.*, vol. 63, no. 12, pp. 5325–5333, Dec. 2015.

[192] P. Xie, G. Wang, H. Li, and J. Liang, "A dual-polarized two-dimensional beam-steering Fabry–Pérot cavity antenna with a reconfigurable partially reflecting surface," *IEEE Antennas Wireless Propag. Lett.*, vol. 16, pp. 2370–2374, 2017.

[193] H. Zhou, A. Pal, A. Mehta, D. Mirshekar-Syahkal, and H. Nakano, "A four-arm circularly polarized high-gain high-tilt beam curl antenna for beam steering applications," *IEEE Antennas Wireless Propag. Lett.*, vol. 17, pp. 1034–1038, 2018.

[194] M. Al Sharkawy and A. A. Kishk, "Wideband beam-scanning circularly polarized inclined slots using ridge gap waveguide," *IEEE Antennas Wireless Propag. Lett.*, vol. 13, pp. 1187–1190, 2014.

[195] H. Liu, S. Gao, and T. H. Loh, "Low-cost beam-switching circularly-polarised antenna using tunable high impedance surface," in *Proc. Loughborough Antennas Propag. Conf. (LAPC)*, Nov. 2012, pp. 1–3.

[196] D.-F. Guan, P. You, Q. Zhang, Z.-H. Lu, S.-W. Yong, and K. Xiao, "A wide-angle and circularly polarized beam-scanning antenna based on microstrip spoof surface plasmon polariton transmission line," *IEEE Antennas Wireless Propag. Lett.*, vol. 16, pp. 2538–2541, 2017.

[197] Y.-Q. Wen, B.-Z. Wang, and X. Ding, "Wide-beam circularly polarized microstrip magnetic-electric dipole antenna for wide-angle scanning phased array," *IEEE Antennas Wireless Propag. Lett.*, vol. 16, pp. 428–431, 2017.

[198] W. Lin, H. Wong, and R. W. Ziolkowski, "Circularly polarized antenna with reconfigurable broadside and conical beams facilitated by a mode switchable feed network," *IEEE Trans. Antennas Propag.*, vol. 66, no. 2, pp. 996–1001, Feb. 2018.

[199] Y.-L. Lyu, F.-Y. Meng, G.-H. Yang, D. Erni, Q. Wu, and K. Wu, "Periodic SIW leaky-wave antenna with large circularly polarized beam scanning range," *IEEE Antennas Wireless Propag. Lett.*, vol. 16, pp. 2493–2496, 2017.

[200] L. Di Palma, A. Clemente, L. Dussopt, R. Sauleau, P. Potier, and P. Pouliguen, "Circularly-polarized reconfigurable transmitarray in Ka-band with beam scanning and polarization switching capabilities," *IEEE Trans. Antennas Propag.*, vol. 65, no. 2, pp. 529–540, Feb. 2017.

[201] M. Karimipour and N. Komjani, "Realization of multiple concurrent beams with independent circular polarizations by holographic reflectarray," *IEEE Trans. Antennas Propag.*, vol. 66, no. 9, pp. 4627–4640, Sep. 2018.

[202] W. W. Li and K. W. Leung, "Omnidirectional circularly polarized dielectric resonator antenna with top-loaded Alford loop for pattern diversity design," *IEEE Trans. Antennas Propag.*, vol. 61, no. 8, pp. 4246–4256, Aug. 2013.

[203] P. Xie, G. Wang, X. Zou, and B. Zong, "Circularly polarized FP resonator antenna with 360° beam-steering," *IEEE Trans. Antennas Propag.*, vol. 69, no. 12, pp. 8854–8859, Dec. 2021.

[204] A. Chen, X. Ning, L. Wang, and Z. Zhang, "A design of radiation pattern and polarization reconfigurable antenna using metasurface," in *Proc. IEEE Asia–Pacific Microw. Conf. (APMC)*, Nov. 2017, pp. 108–111.

[205] Y. Zhang, S. Lin, Y. Li, J. Cui, F. Dai, J. Jiao, and A. Denisov, "Wideband pattern- and polarization-reconfigurable antenna based on bistable composite cylindrical shells," *IEEE Access*, vol. 8, pp. 66777–66787, 2020.

[206] S.-L. Chen, D. K. Karmokar, P.-Y. Qin, R. W. Ziolkowski, and Y. J. Guo, "Polarization-reconfigurable leaky-wave antenna with continuous beam scanning through broadside," *IEEE Trans. Antennas Propag.*, vol. 68, no. 1, pp. 121–133, Jan. 2020.

[207] M. Allayioti, J. R. Kelly, and R. Mittra, "Beam and polarization reconfigurable microstrip antenna based on parasitics," *Microw. Opt. Technol. Lett.*, vol. 60, no. 6, pp. 1460–1464, Jun. 2018.
[208] X. Yuan, Z. Li, D. Rodrigo, H. S. Mopidevi, O. Kaynar, L. Jofre, and B. A. Cetiner, "A parasitic layer-based reconfigurable antenna design by multi-objective optimization," *IEEE Trans. Antennas Propag.*, vol. 60, no. 6, pp. 2690–2701, Jun. 2012.
[209] X.-S. Yang, B.-Z. Wang, S. H. Yeung, Q. Xue, and K. F. Man, "Circularly polarized reconfigurable crossed-yagi patch antenna," *IEEE Antennas Propag. Mag.*, vol. 53, no. 5, pp. 65–80, Oct. 2011.
[210] W. Li, Y. M. Wang, Y. Hei, B. Li, and X. Shi, "A compact low-profile reconfigurable metasurface antenna with polarization and pattern diversities," *IEEE Antennas Wireless Propag. Lett.*, vol. 20, no. 7, pp. 1170–1174, Apr. 2021.
[211] G.-W. Yang, J. Li, B. Cao, D. Wei, S.-G. Zhou, and J. Deng, "A compact reconfigurable microstrip antenna with multidirectional beam and multipolarization," *IEEE Trans. Antennas Propag.*, vol. 67, no. 2, pp. 1358–1363, Feb. 2019.
[212] M. Chen, H. Hu, S. Lei, K. Sun, J. Tian, and B. Chen, "A 3-D pattern reconfigurable antenna array with multi-polarization," *IEEE Antennas Wireless Propag. Lett.*, vol. 22, no. 9, pp. 2105–2109, May 2023.

VENKATASWAMY SURYAPAGA (Student Member, IEEE) received the B.Tech. degree in electronics and communication engineering from Bapatla Engineering College, Bapatla, Andhra Pradesh, India, in 2004, and the M.Tech. degree in digital electronics and communication systems from the QIS College of Engineering, Ongole, Andhra Pradesh, in 2010. He is currently an Internal Full-Time Research Scholar with the School of Electronics Engineering (SENSE), VIT-AP University, Amaravati, Andhra Pradesh. His research interest includes design of reconfigurable antennas using metamaterials for 5G and beyond applications.

VIKAS V. KHAIRNAR (Member, IEEE) received the B.E. degree in electronics and telecommunication engineering from Savitribai Phule Pune University, India, in 2009, the M.E. degree in communication engineering from Dr. BAMU University, India, in 2013, and the Ph.D. degree from BITS Pilani, India, in 2020. He is currently an Assistant Professor with the School of Electronics Engineering (SENSE), VIT-AP University, Amaravati, Andhra Pradesh, India. His research interests include the design of reconfigurable antennas, antenna arrays, and metasurface inspired antennas.